

An Experimental Investigation of the Effect of Rust and Mechanical damage on the Maximum Experimental Safe Gap for Ethylene Gas Explosions

Marianne Winnes Steiner

A thesis submitted in partial fulfillment of the
requirements for the degree of Master of Science in
the subject of Physics; Process Safety Technology



Department of Physics and Technology

University of Bergen

Bergen Norway

June 2012

Acknowledgements

This thesis is a part of the master program in Process Technology at The University of Bergen, Department of Physics and Technology. The experimental work has been performed in the Gas Explosion Laboratory at the UoB.

First I would like to thank my supervisors, Associate Professor Bjørn J. Arntzen and Professor Rolf K. Eckhoff, for the guidance, advice and good discussions they have provided me throughout the work on this thesis.

Thanks to Leif Egil Sandnes at the Mechanical Workshop who helped in making parts to the experimental apparatus. Chief engineer at the Section of Microelectronic at UoB, Werner Olsen, helped when problems with electrical equipment occurred. Also thanks to Marte Henden who taught me how the gas analyzer is used.

I would also like to acknowledge the good cooperation I had with Linn Ringdal and Eivin Larsen in sharing the same experimental apparatus and helping each other when problems arose. They have also provided good discussions that have been of assistance during the work with this thesis. Also thanks to other fellow master students who have contributed to a good working environment in the office

I would like to thank my good friend Astrid S. Skårdalmo for reading through my draft and giving me useful feedback and corrections.

A special thanks to master student Linn Ringdal who has been my fellow student and good friend throughout our studies. Her friendship has made our five years of higher education an unforgettable time.

Thanks to my good friend Caroline Grønneberg whose support and encouragement have been invaluable when living far away from my family. Also thanks to my loyal friends back home for always caring for me, even though times spent on studies and in Bergen have been longer than times spent in their company.

My family back home deserves special thanks for always making me feel welcome when I came home to visit, and for always caring and showing interest in my life as a student.

Finally, I would like to express my deepest gratitude to my parents Gro W. Steiner and Lasse Steiner whose love, dedication and many years of support has brought me this far. Their encouragement, genuine interest and financial support make me forever grateful.



Department of Physics and Technology
University of Bergen
Norway

Abstract

Gas explosions are a great hazard in the industry where flammable substances are handled. Engines, switches and other electrical equipment can act like ignition sources where an explosive atmosphere is present. Possible ignition sources are placed in flameproof enclosures which are designed to withstand an internal explosion and prevent transmission of hot combustion products to ignite an explosive outer atmosphere. All flameproof enclosures have to fulfill the requirements given by the international standard. The current international standard (IEC 2011) require that the maximal average roughness (R_a) of a flame gap surface is $\leq 6.3\mu\text{m}$. Any damaged flame gap must be brought back to its original state.

The current standard (IEC) gives no technical argument to justify the requirements of an average roughness $\leq 6.3\mu\text{m}$. Previous experimental work (Grosvik 2010; Opsvik 2010; Solheim 2010) has shown that the gap efficiency has in fact improved when applying rust and mechanical damage to the flame gap surfaces so that the average roughness is greater than $6.3\mu\text{m}$. In those experiments, propane has been used as the test gas. The purpose of the present experimental work is to investigate what effect rust and mechanical damage have on the efficiency of the flame gap to prevent a re-ignition of an explosive ethylene/air mixture. Ethylene is a highly reactive gas.

The maximum experimental safe gap (MESG) of an explosive gas mixture is the largest gap width which prevents transmission of an internal explosion to the external atmosphere. The MESG is usually used to compare different gases. In the present investigation the MESG is used as parameter to compare how different damages affect the MESG value compared to an undamaged flame gap. If the MESG increases it means that gap efficiency increases, and if the MESG decreases the gap efficiency decreases.

All of the experiments in the present work were performed in the Plane Rectangular Slit Apparatus with ethylene as the test gas.

Flame gaps were explosion tested before and after rusting. The results showed a decrease in the number of re-ignitions after corrosion. None of the rusted slits gave re-ignition on the first explosion test, which is the most important. The main conclusion is that rust increased the efficiency of the flame gap to prevent a re-ignition in the secondary chamber.

Experiments on mechanically milled crosswise grooves with different depth showed that the MESG value increased for the slits with the deepest grooves. One slit which had the smallest value of depth, had the same MESG value as for an undamaged slit. This means that crosswise grooves did not reduce the efficiency of the gap, and that the slit with deepest grooves in fact increased the efficiency.

The overall conclusion from this experimental work is that surface roughness above the requirement given by the IEC standard does not reduce the efficiency of the flame gap for an internal ethylene gas explosion.

Table of Contents

Acknowledgements	I
Abstract	II
Table of Contents	III
1 Introduction.....	- 1 -
1.1 Background.....	- 1 -
1.2 Motivation	- 2 -
2 Review of Relevant Literature	- 3 -
2.1 Gas Explosions	- 3 -
2.1.1 Radical chain reactions.....	- 3 -
2.1.2 Laminar flame speed and burning velocity	- 4 -
2.1.3 Ignition	- 6 -
2.1.4 Flammable limit	- 7 -
2.1.5 Gas groups.....	- 7 -
2.1.6 Zone classification.....	- 8 -
2.2 Flameproof enclosure (Ex'd'').....	- 9 -
2.2.1 The concept of flameproof enclosure.....	- 9 -
2.2.2 Requirements given by the IEC	- 9 -
2.2.3 Damages on Ex'd' equipment.....	- 10 -
2.3 Explosion transmission through narrow gaps.....	- 11 -
2.3.1 Maximum Experimental Safe Gap, MESG.....	- 11 -
2.3.2 Quenching of flame by a cold wall	- 12 -
2.3.3 Heat transfer to gap wall	- 13 -
2.3.4 Wall roughness and friction factor	- 15 -
2.3.5 Effect of roughness on heat transfer.....	- 17 -
2.3.6 Ignition by a jet of hot combustion products.....	- 17 -

2.3.7	Cooling from entrainment and mixing with cold unburned gas in the external chamber - 19 -	
2.4	Previous experimental research on explosion transmission through narrow gaps - 20 -	
2.4.1	H. Phillips work.....	- 20 -
2.4.2	T. Redeker	- 22 -
2.4.3	Ø. Larsen	- 24 -
2.4.4	H.E.Z. Opsvik.....	- 27 -
2.4.5	A. Grov.....	- 27 -
2.4.6	F. Solheim	- 29 -
2.5	Basic corrosion theory	- 32 -
2.6	Ethylene	- 34 -
3	Experimental Procedures and Apparatus	- 35 -
3.1	Overall experimental approach.....	- 35 -
3.2	The Plane Rectangular Slit Apparatus	- 36 -
3.2.1	Slits.....	- 37 -
3.2.2	Direction of the flow in the primary chamber	- 40 -
3.2.3	Adjustment of the ignition position.....	- 40 -
3.2.4	Adjustment of the thermocouple position	- 41 -
3.3	Different experiments carried out.....	- 42 -
3.3.1	Rusted gap surface	- 42 -
3.3.2	The most dangerous concentration of ethylene for re-ignition in the secondary chamber - 43 -	
3.3.3	Optimal ignition position for re-ignition in the secondary chamber with undamaged slits and the MESG.....	- 43 -
3.3.4	Optimal ignition position for re-ignition in the secondary chamber for slits with seven crosswise grooves	- 44 -
3.3.5	Flame gap surfaces with different depths on the multiple crosswise grooves-	44 -
	-	
3.4	The Servomex 4200 Industrial Gases Analyser	- 45 -

3.5	Measurement system and spark triggering	- 45 -
3.5.1	Pressure measurements	- 45 -
3.5.2	Temperature measurements.....	- 45 -
3.6	Sources of Error.....	- 47 -
3.6.1	Data Acquisition system.....	- 47 -
3.6.2	Gas concentration measurements	- 47 -
3.6.3	Air humidity	- 47 -
3.6.4	Pressure	- 47 -
3.6.5	Temperature	- 47 -
3.6.6	Condensed water	- 48 -
3.6.7	Experiments.....	- 48 -
4	Experimental Results and Discussion.....	- 49 -
4.1	Experiments on rusted flame gap surfaces	- 49 -
4.1.1	Results	- 49 -
4.1.2	Discussion	- 52 -
4.2	Experiments to find the most dangerous concentration of ethylene for re-ignition in the secondary chamber	- 54 -
4.2.1	Results	- 54 -
4.2.2	Discussion	- 55 -
4.3	Experiments to find the optimal ignition position for re-ignition in the secondary chamber with undamaged slits, and the MESG for ethylene	- 56 -
4.3.1	Results	- 56 -
4.3.2	Discussion	- 58 -
4.4	Experiments to find the optimal ignition position for re-ignition in the secondary chamber for slits with seven crosswise grooves.....	- 60 -
4.4.1	Results	- 60 -
4.4.2	Discussion	- 63 -
4.5	Experiments with different depths on the multiple crosswise grooves	- 65 -

4.5.1	Results	- 65 -
4.5.2	Discussion	- 67 -
5	Conclusion	- 69 -
6	Recommendations for Further Work	- 71 -
	References	- 73 -
Appendix A	Experimental apparatus and procedures	i
A-1	Equipment data	i
A-2	Experimental procedure - The Plane Rectangular Slit Apparatus	ii
A-2.1	Adjusting Procedure-gap opening in the PRSA	ii
A-2.2	Experimental procedure	iv
A-2.3	Calibration procedure	v
A-2.4	Data Acquisition System	vi
Appendix B	Calculations	ix
B-1	Calculation of vol. % O ₂ in a mixture of ethylene and air	ix
B-2	Calculation of flow ethylene into the PRSA	xi
Appendix C	Experimental equipment	xii
C-1	High speed camera	xii
C-2	Thermocouples	xii
Appendix D	Different measurement data from experiments performed in the present work	xiv

1 Introduction

1.1 Background

Hydrocarbon leaks have a major accident potential, and the latest big disaster to illustrate this is the Deep Water Horizon accident in the Mexico Gulf. The explosion was caused by a blow out from the well head which led to methane gas into the ventilation plant. The methane was ignited and caused a series of subsequent explosions on the platform. 11 persons were killed, and the platform sank.

Studying the mechanism of explosions can provide knowledge on how to prevent accidents. In 2003 the Norwegian authorities took an initiative to reduce the number of leaks. The aim was to cut the number of hydrocarbon leaks larger than 0.1 kg/s by 50 percent before the end of 2005, using the average for 2000-2002 as its baseline. Figure 1-1 shows the number of hydrocarbon leaks on Norwegian installations from year 2000-2009.

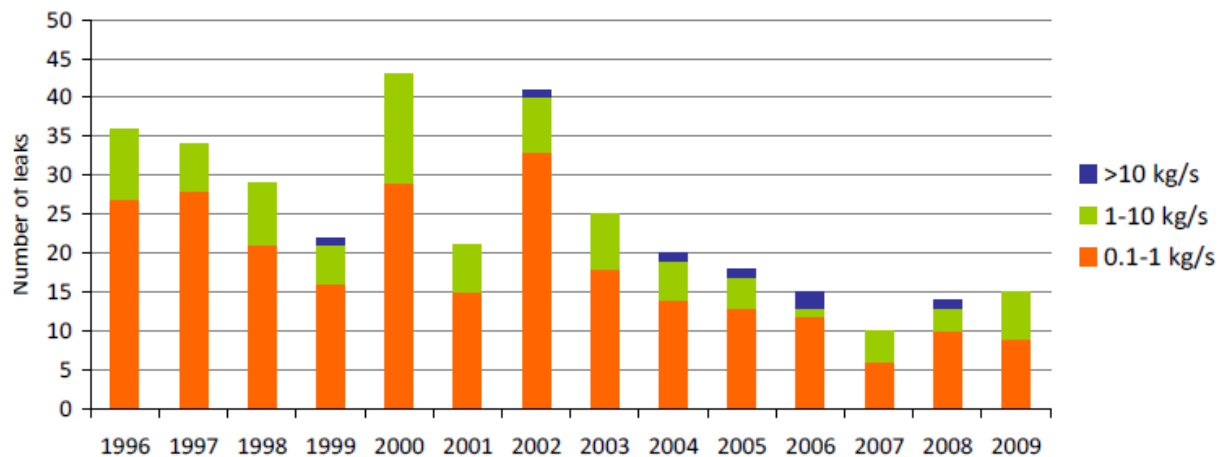


Figure 1-1 Hydrocarbon leaks on Norwegian installations in the period 2000 to 2009. All leaks are above 0.1 Kg/s. From (Petroleum Safety Authority Norway 2009)

Although the number of leaks through the years has decreased, there is a risk of gas explosions to occur if an ignition source is present. It is therefore important to have control over possible ignition sources, e.g electrical equipment. The use of electrical equipment where a possible explosive atmosphere is present, demands special protection. Requirements for the protection equipment are regulated by international standards.

One type of protection method is the flameproof enclosure (Ex"d"). This method is used to keep potential electrical ignition sources and hot surfaces inside a protective enclosure. The enclosure has to withstand the pressure from an internal explosion, and prevent hot combustion products vented through holes and slits from igniting an explosive atmosphere outside it.

1.2 Motivation

Ex”d” protection equipment is widely used in the offshore industry, where formation of rust is a potential damage. International Electrotechnical Committee (IEC) requires an average surface roughness of the joints to be $< 6.3\mu\text{m}$. All damaged equipment has to be brought back to its originally state. A consequence of these regulations is that a considerable amount of resources are used on maintenance. The IEC does not provide any guidance as to what extent of damage is considered to reduce the efficiency of the gap.

The aim of this experimental research is to investigate how mechanical damage and rust with a greater average roughness than $6.3\mu\text{m}$ affect the gap efficiency for ethylene gas explosions. This work is a continuation of the work performed by (Solheim 2010), (Grosv 2010) and (Opsvik 2010) where they showed that adding damage to the flame gap did in most cases improve the efficiency of the gap. They used propane as the test gas. Ethylene is more reactive gas, and ethylene gas explosions may be more sensitive to changes in the gap surface configuration.

2 Review of Relevant Literature

2.1 Gas Explosions

The term “explosion” has many definitions in the literature, but mainly they can be divided into two categories. One focuses on the noise due to sudden release of a strong pressure wave, and the other considers the sudden release of chemical energy. Eckhoff (Eckhoff 2005) propose this definition to an explosion: “An explosion is an exothermal chemical process that, when occurring at constant volume, gives rise to a sudden and significant pressurize”.

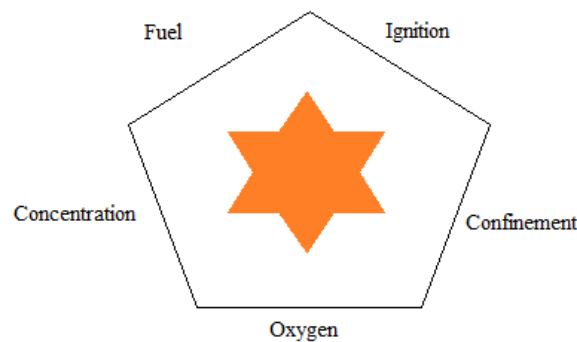


Figure 2-1 Explosion pentagon

An explosion may occur when flammable gas or liquid is mixed with air within certain concentrations, and are exposed to an ignition source. Figure 2-1 illustrates the requirements to get a chemical gas or liquid explosion:

1. Fuel: combustible gas, vapor, mist or dust
2. Oxidizer: oxygen or air
3. Concentration has to be within the flammable limit
4. Confinement necessary for pressurize
5. Ignition source

2.1.1 Radical chain reactions

A combustion process is formed by radical chain reactions. A radical is an atom, molecule or ion with unpaired electrons on an open shell configuration. The unpaired electrons make radicals highly reactive because they seek stability.

The general principle for a radical chain reaction can be demonstrated by using the hydrogen-oxygen system shown in Table 2-1 (Warnatz, Maas et al. 2006).

Table 2-1 Radical chain reactions. Based on (Warnatz, Maas et al. 2006)

a	$H_2 + O_2 = 2OH\cdot$	chain initiation
b	$OH\cdot + H_2 = H_2O + H\cdot$	chain propagation
c	$H\cdot + O_2 = OH\cdot + O\cdot$	chain branching
d	$H\cdot = \frac{1}{2} H_2$	chain termination

In the chain initiation step the reactive species are formed from stable species. The reactive intermediate species react with other stable species in the chain propagation step. When a radical and a stable species forms two reactive species, the step is called chain branching. The last step, the chain termination, is when the reactive species react to stable species.

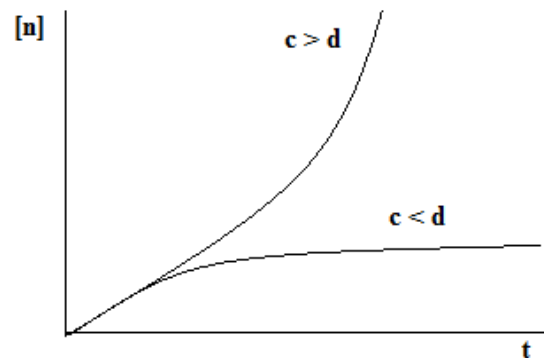


Figure 2-2 Development of intermediate radicals. Based on (Warnatz, Maas et al. 2006)

If a reaction has more chain branching steps (c) than chain termination steps (d), $c > d$, the concentration $[n]$ of radicals will increase exponential with time, which will lead to an explosion. If $c < d$, a time independent stationary solution is obtained, and there will be no explosion. See Figure 2-2.

2.1.2 Laminar flame speed and burning velocity

Laminar flame speed S_f is defined as the propagation velocity of flame a through a quiescent gas, normal to the flame front into the reactants. The burning velocity, S_u is the velocity by which the combustion reaction is “eating” itself into the unburned gas/air mixture. The relation between the flame speed and the burning velocity is:

$$S_f = S_u + S_g \quad 2-1$$

Where S_g is the velocity of the unburned gas. (Bjerketvedt, Bakke et al. 1997; Eckhoff 2005)

When a gas cloud is ignited by a relatively weak ignition source, like an electrical spark, the flame starts as a laminar flame. The basic mechanism of propagation of a laminar flame is molecular diffusion of heat and mass. The laminar flame speed depends on the type of fuel and concentration. Figure 2-3 shows the laminar burning velocity of methane, ethylene and hydrogen in air. Methane has a maximum laminar burning velocity of about 0.4 m/s. Ethylene and hydrogen has higher laminar burning velocities due to faster chemical kinetics and higher molecular diffusivities. The laminar burning velocities may vary with type of apparatus and measurement systems. (Bjerketvedt, Bakke et al. 1997)

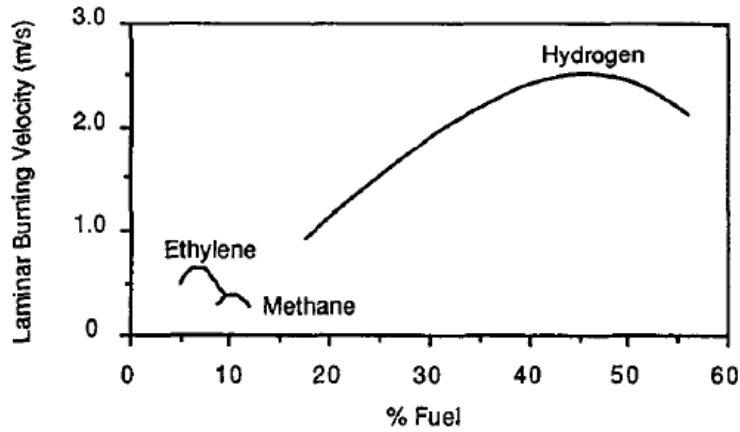


Figure 2-3 Laminar burning velocity of methane- ethylene- and hydrogen -air. From (Bjerketvedt, Bakke et al. 1997).

Figure 2-4 shows the relationship between the laminar burning velocity and fraction of stoichiometric concentration for some other fuels. All of the hydrocarbons mixed with air have maximum laminar burning velocities slightly above the stoichiometric value.

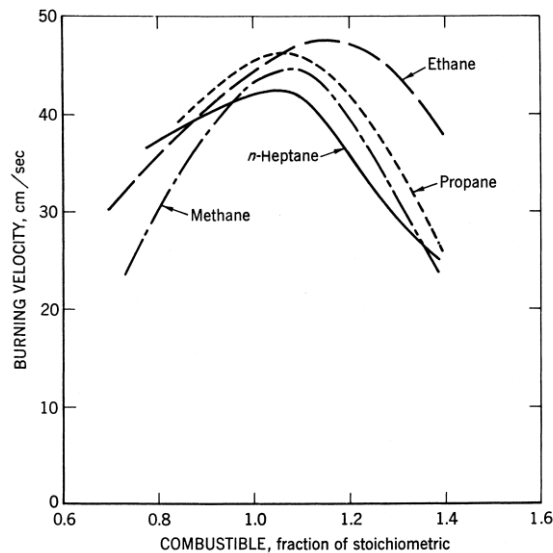


Figure 2-4 Laminar burning velocities S_u at atmospheric pressure and temperature for mixtures of various hydrocarbon gases and air. From (Zabetakis 1965).

Table 2-2 shows the maximum laminar burning velocities for some premixed fuel/air mixtures.

Table 2-2 Maximum laminar burning velocities S_u for premixed fuel/air at atmospheric pressure and normal temperature for some fuels. From (Eckhoff 2005)

Fuel	Maximum S_u [cm/s]
Alkanes	40-50
Ethylene	75
Hydrogen	325

2.1.3 Ignition

The location and strength of the ignition source are important factors in how a gas explosion develops. Most likely the ignition source is a weak spark or a hot surface. Figure 2-5 illustrates two ignition scenarios. When the gas is ignited close to the vent area the combustion products will be vented and the flow velocity in the unburnt mixture will be low. An ignition in the closed end of a tube will give rise to a high flow velocity ahead of the flame. The lowest pressure is obtained if the ignition point is close to the vent area. (Bjerketvedt, Bakke et al. 1997)

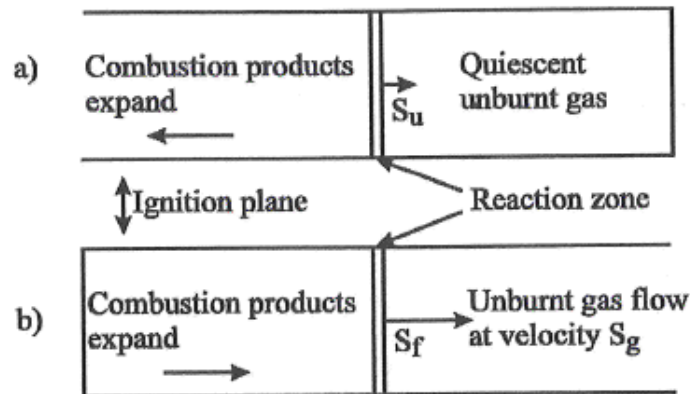


Figure 2-5 Effect of different ignition locations in a compartment. From (Eckhoff 2005)

Figure 2-6 shows Schlieren photographs of two explosions in a 1 liter primary chamber where the combustion products are vented through a nozzle at the top of the chamber and into a secondary chamber. When the ignition source is placed in the center a spherical flame develops throughout the volume which eventually hits the vertical walls of the chamber. An ignition close to the vent area leads to an earlier interruption of the flame front by the head of the chamber and the flame propagates downwards in the chamber.

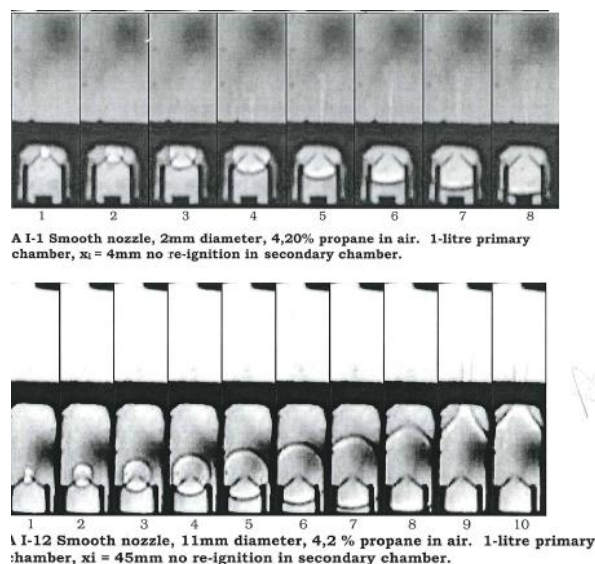


Figure 2-6 Schlieren photographs of explosions in a 1 liter primary chamber. From (Einarsen 2001)

2.1.4 Flammable limit

A combustible mixture can only be ignited if it is between the lower and upper flammable limit, i.e. LFL and UFL. The flammable limits for a mixture of gas/vapor in air are often given in volumetric percent or g/m^3 . If the concentration is below the LFL, the mixture is too lean to be ignited, and if it is above the UFL the mixture is too rich. The flammability limits are found experimentally, and standard test conditions are 25°C and 1 atm (Bjerketvedt, Bakke et al. 1997). Flammability limits for some combustible gases and vapors in air are listed in Table 2-3, along with the minimum ignition temperature.

Table 2-3 Flammable limits and minimum ignition temperature for some combustible gases and vapors in air at atmospheric pressure and normal temperature. Based on (Eckhoff 2005).

Fuel	Flammable limits [vol. % in air]		Min. ign. temp [°C]
	Lower	Upper	
Ethane	3	12.4	515
Ethylene	2.7	36	425
Hydrogen	4	75	560
Propane	2.1	9.5	493

2.1.5 Gas groups

Inflammable gases and vapors are classified into the group or sub-group of equipment required for use in the current gas or vapor atmosphere.

The groups of equipment for explosive gas atmospheres are, according to (IEC 2010) :

- Group I: equipment for mines where there is firedamp
- Group II: equipment for places with an explosive gas atmosphere other than mines

Group II is divided into three sub-groups, A, B and C. The gases and vapors are classified according to their maximum experimental safe gap (MESG) or their minimum igniting current (MIC). Table 2-4 shows the limits for MESG and MIC given by the (IEC 2010) .

Table 2-4 Group limits for MESG and MIC for classification of gases and vapor.

Group	MESG	MIC
Group IIA	MESG < 0.9 mm	MIC > 0.8
Group IIB	0.5 mm < MESG < 0.9 mm	0.45 ≤ MIC ≤ 0.8
Group IIC	MESG ≤ 0.5 mm	MIC < 0.45

Table 2-5 shows some gases, with their respective gas groups, typically used in the offshore industry.

Table 2-5 Gas Groups. Based on (Elsebutangen 1997).

Gas group	Example of gas
IIA	Methane, ethane, propane
IIB	Ethylene, hydrogen sulphide
IIC	Hydrogen, acetylene

In this present work ethylene is used as the test gas. Ethylene is classified as Group IIB gas. Previous experimental work on rusted and mechanical damaged flame gaps has been investigated with a group IIA gas.

2.1.6 Zone classification

The basis that forms the requirements for the equipment used in explosive atmosphere is area classification (Elsebutangen 1997). The aim is to minimize the probability of ignition by dividing an area into different zones with regards to the occurrence of an explosive atmosphere. According to (Eckhoff 2005) these zones are defined as;

- Zone 0: Part of the hazardous area in which a flammable atmosphere is continuously present or present for long periods.
- Zone 1: Part of a hazardous area in which a flammable atmosphere is likely to occur in normal operation.
- Zone 2: Part of a hazardous area in which a flammable atmosphere is not likely to occur in normal operation, and if it occurs it exists only for a short period.

A series of standardized basic design concepts for equipment used in such hazardous areas have existed for a long time. The most common ones are (Eckhoff 2005):

- Intrinsic safety (Ex 'i')
- Flame Proof Enclosure (Ex 'd')
- Increased Safety (Ex 'e')
- Pressurized Apparatus (Ex 'p')
- Oil-Filled Enclosures (Ex 'o')
- Sand-Filled Enclosures (Ex 'q')
- Encapsulation (Ex 'm')

Investigations of flameproof enclosures are conducted in this present work.

2.2 Flameproof enclosure (Ex”d”)

2.2.1 The concept of flameproof enclosure

The purpose of a flameproof enclosure is to prevent an accidental internal explosion igniting an explosive atmosphere outside the enclosure. Possible ignition sources, such as engines and electrical switches, are placed in the enclosure which has to withstand the explosion pressure, and efficiently cool the hot gas vented through the joints. An illustration of a flameproof enclosure is given in Figure 2-7.

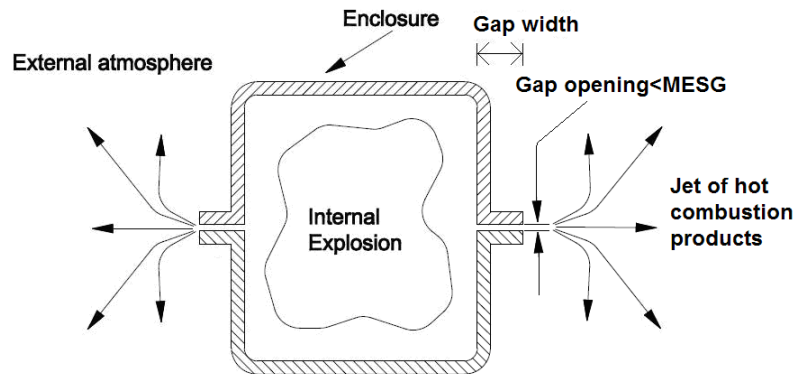


Figure 2-7 Illustration of flameproof enclosure with an internal explosion. From (Opsvik 2010)

There are several different types of joints used in flameproof equipment such as flat flange joints, spigot joints, cylindrical joints, operating rod joints and partial cylindrical joints. Flat flange joints are studied in this experimental work.

2.2.2 Requirements given by the IEC

The International Electrotechnical Commission (IEC) is the world’s leading organization for the preparation and publication of International Standards for all electrical, electronic and related technologies. It was officially founded in 1906 as a result of the need for standards and regulations when engineers and scientists struggled with chaos on emerging discoveries in the electrical industry over the 19th century.

Flameproof enclosures need to fulfill the requirements given by the IEC. Transmission of an explosion inside the enclosure to the external atmosphere is prevented if the gap between the plain parallel flange surfaces is less than the maximum experimental safe gap, MESG. MESG is defined by the (IEC 2011) as the maximum gap of a joint of 25 mm in width which prevents any transmission of an explosion during 10 tests made under the conditions in IEC 60079-20-1. MESG is described in more detail in section 2.3.1. IEC requires that the surfaces of joints in the gap “shall be such that their average roughness R_a does not exceed $6.3\mu\text{m}$ ”. A damaged gap must be brought back to its original state.

Some other requirements are:

- The temperature of the external surface shall not exceed the minimum ignition temperature of the surrounding gas.

- The width of joints shall not be less than the minimum values given in Table 2 and 3 in IEC 60079-1 (IEC 2011).

2.2.3 Damages on Ex'd' equipment

Damages on equipment used in the industry may have severe consequences when it disturbs the function of the safety equipment and it is important to have good routines on inspection and maintenance.

The risk of damaging safety equipment is high in the offshore industry. Rust is a problem because the equipment is placed in an environment perfect for corrosion. Flameproof enclosure is mainly made of steel, stainless steel and bronze alloy. Drilling fluids consist of chemicals that absorb water, which have damaging effects on equipment. High pressure cleaner may lead to moist inside the enclosure and can cause rust and short circuit in the electrical equipment. Other damages can be:

- Sparkles from welding, cutting
- Sand blasting can destroy equipment.
- Poor handling of tools under inspection

The IEC standard requires an average roughness of no more than 6.3 μm for flame gaps. All the actions mentioned above can cause a roughness greater than this. The IEC standard does not provide any guidance as to what is considered significant damage that can cause an effect on the efficiency of the safe gap. The present work is an investigation of how different damages with roughness greater than the requirement given by the IEC affect the gap efficiency.

2.3 Explosion transmission through narrow gaps

2.3.1 Maximum Experimental Safe Gap, MESG

Maximum experimental safe gap is the largest gap an enclosure can have so that hot combustion products from an internal explosion do not ignite an external explosive atmosphere. The explosion inside a chamber vented through a narrow gap, may cause a hot jet due to the pressure rise inside the chamber during the explosion. This hot jet may lead to a re-ignition outside the chamber if the atmosphere is explosive and the MESG is not sufficient.

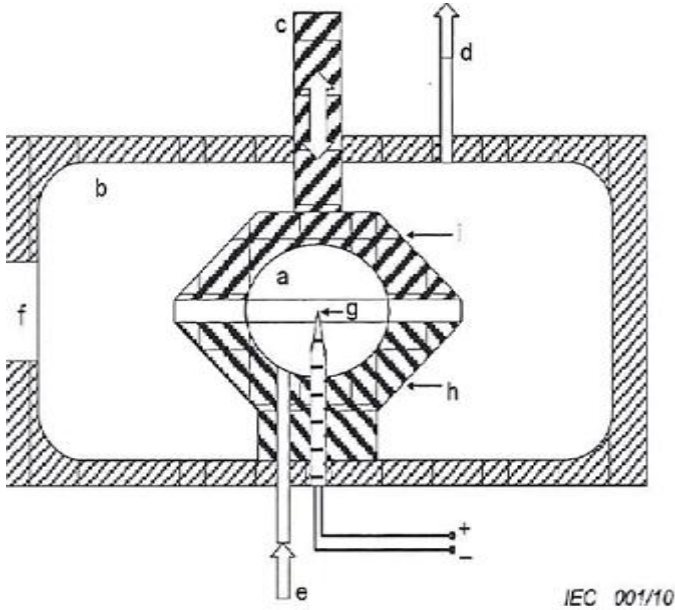


Figure 2-8 Test apparatus for determining MESG. From (IEC 2010).

The standardized test apparatus developed by The International Electrotechnical Commission (IEC) is shown in Figure 2-8. The internal and external chambers are filled with a known mixture of the gas or vapor in air, under normal conditions, 20°C and 100kPa. The circumferential gap between the two chambers is adjusted to desired value. The internal mixture is ignited by the ignition source placed in the center of the internal chamber, and the flame propagation is observed through the window in the external chamber. Maximum experimental safe gap for the gas/vapor is determined by adjusting the gap size in small steps until the gap prevents re-ignition. The largest gap giving no re-ignitions in 10 subsequent experiments is defined as the MESG value for the tested gas/vapor (IEC 2010).

The internal chamber has a volume of 20 cm³ and the external cylindrical chamber has a diameter of 200 mm and a height of 75 mm. The apparatus is constructed to withstand a maximum pressure of 1500 kPa. To obtain accurate and valid results, the flow of the mixture is maintained until the inlet and outlet concentration is the same (IEC 2010).

MESG varies with type of gas. MESG values for some combustible gases and vapors are listed in Table 2-6. From Figure 2-9 it is seen that the safe gaps varies with the concentration of fuel in air. The smallest safe gap is referred to as the MESG.

Table 2-6 MESG values for some combustible gases and vapors in air at atmospheric pressure and normal temperature. From (Eckhoff 2005).

Fuel	MESG [mm]
Ethylene	0.65
Heptane	0.91
Hydrogen	0.28
Methane	0.14
Propane	0.92

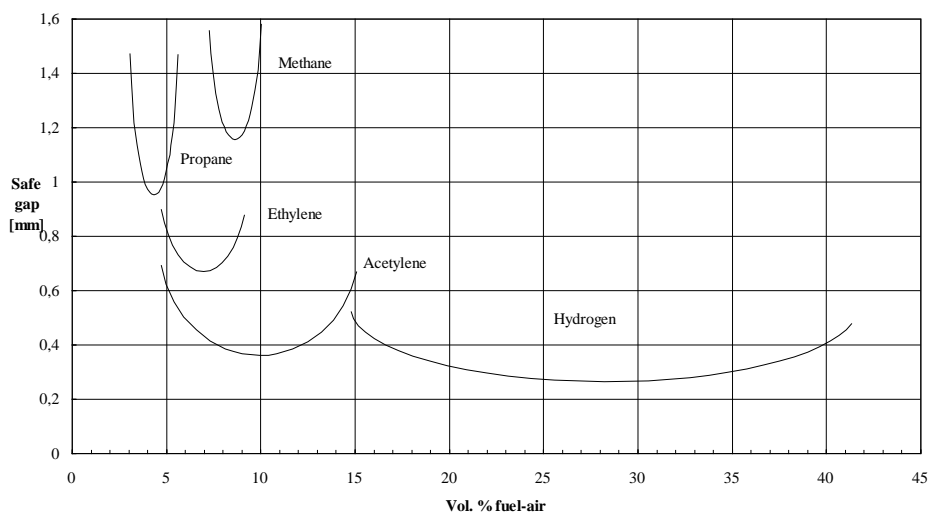


Figure 2-9 Safe gap as a function of vol. % fuel-air for different gases. The lowest points on the curves are referred to as the MESG. From (Beyer 1996).

2.3.2 Quenching of flame by a cold wall

Flames will extinguish when they enter a sufficiently small passageway. If the passageway is not small enough, the flames will propagate through it. (Turns 2012) defines the quenching distance as:

“The critical diameter of a circular tube where a flame extinguishes rather than propagates”.

For other dimensions, such as flat flange joints, the quenching distance is the width of the gap opening.

The quenching distance must not be confused by the MESG. The QD is, according to (Eckhoff 2005), roughly given as:

$$QD = 2 \cdot MESG$$

2-2

(Williams 1985) provides a thumb rule applicable to the problem of flame quenching by a cold wall:

“The rate of liberation of heat by chemical reactions inside the slab must approximately balance the rate of heat loss from the slab by thermal conduction. “

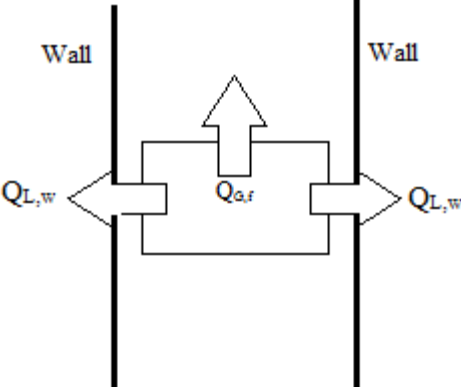


Figure 2-10 Flame quenching between two parallel walls. Based on (Turns 2012).

Figure 2-10 illustrates a flame propagating through two parallel walls. By applying Williams’ criterion, we can write a simplified energy balance by equating the heat production to the heat lost by conduction to the walls (Turns 2012):

$$\dot{Q}_{G,f}V = \dot{Q}_{L,w} \tag{2-3}$$

$\dot{Q}_{G,f}$ = the volumetric heat release rate from the flame

$\dot{Q}_{L,w}$ = the heat loss due to conduction to the walls

This simplified model does not take heat loss due to convection into account.

2.3.3 Heat transfer to gap wall

When hot combustion products flows through a channel, heat transfer between the “cold” wall and the combustion products will occur. In this section the basic mechanism of heat transfer from a hot fluid to a cold surface is described.

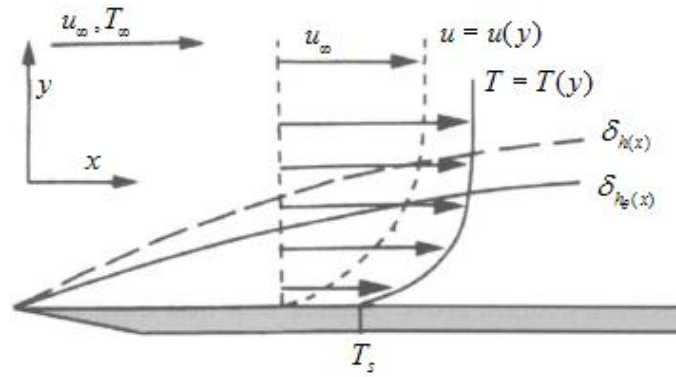


Figure 2-11 The dashed line shows the hydrodynamic boundary layer, and the solid line shows the thermal boundary layer. From (Kanury 1975).

Consider Figure 2-11. A fluid flows with bulk velocity u_∞ with a bulk temperature T_∞ . The part of the moving fluid that is influenced by the presence of a solid boundary is called the boundary layer. This is where the heat transfer occurs. The velocity of the fluid is zero at the interface and increases to its bulk velocity further away from the wall. This is called the hydrodynamic boundary layer. The thermal boundary layer is the temperature difference from wall to bulk. The fluid temperature is equal to the surface temperature of the solid at the interface and increases to bulk temperature at a given distance from the wall.

Fourier's law is known as the law of heat conduction where the flux is proportional to the temperature gradient and opposite to it in sign. (McCabe, Harriott et al. 2005). For one-dimensional heat flow it is given by:

$$\frac{dq}{dA} = -k \frac{dT}{dx} \quad 2-4$$

Where: q = rate of heat flow in direction normal to surface

A = surface area

T = Temperature

x = distance normal to surface

k = proportionality constant or thermal conductivity

The convective heat transfer due to movement in the fluid is given by Newton's law of cooling. (McCabe, Harriott et al. 2005):

$$\frac{q}{A} = h(T_s - T_f) \quad 2-5$$

Where: T_s = surface temperature
 T_f = bulk temperature
 h = heat transfer coefficient

If a fluid is without any motion, heat transfer occurs only by conduction, but the faster the fluid moves, the greater is the heat transfer by convection. The Nusselt number gives a ratio of convective to conductive heat across the boundary layer and a large Nusselt number suggest that the heat transfer is mainly due to convection.

$$Nu = \frac{hl}{k} \quad 2-6$$

Where: l = the characteristic dimension of the surface
 k = the thermal conductivity of the fluid
 h = the convective heat transfer coefficient

The Prandtl number characterizes the regime of convection in the boundary layer.

$$Pr = \frac{\nu}{\alpha} \quad 2-7$$

Where: ν = kinematic viscosity
 α = thermal diffusivity

When $Pr \gg 1$, the thermal boundary layer lies within the hydrodynamic boundary layer. If $Pr \ll 1$, the thermal boundary layer is thicker than the hydrodynamic boundary layer. The Prandtl number is dependent on the fluid and the fluid state, and almost independent of temperature. The Prandtl number is found in property tables.

2.3.4 Wall roughness and friction factor

Surface roughness has an effect on the fluid flow through pipes and channels. The roughness element will cause fluctuations in the boundary layer and lead to turbulence in the flow. Figure 2-12 shows some idealized types of roughness. The height, k , of a single unit roughness is called the roughness parameter, and D is the diameter of the tube which extends to the bottom of the grooves. If the cross section is non-circular the hydraulic diameter has to be used. This also accounts for the following equations given in this section. The relative roughness, ζ , is the ratio between k and D as shown in Equation 2-8. (McCabe, Smith et al. 2005).

$$\xi = \frac{k}{D}$$

2-8

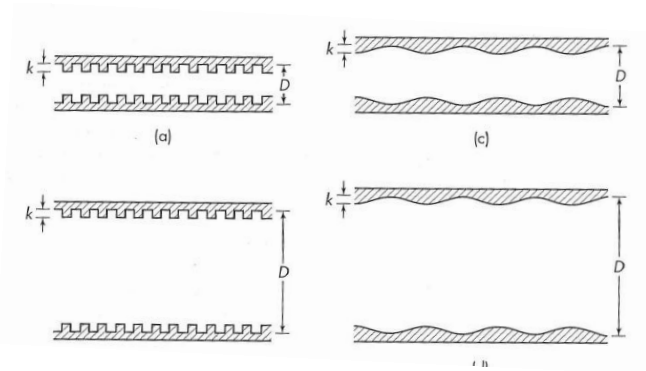


Figure 2-12 Types of roughness. From (McCabe, Smith et al. 2005)

An increased roughness will lead to a higher friction factor. Dimensional analyses show that Fanning friction factor, f , is a function of the relative roughness and the Reynolds number. The Fanning friction factor is given by:

$$f = \frac{2\tau_w}{\rho\bar{V}^2} \quad 2-9$$

Where: τ_w = wall shear stress

ρ = density

\bar{V} = average velocity

The Reynolds number is a dimensionless group of variables, which measures the transition from laminar to turbulent flow. The Reynolds number for a flow in a circular pipe is given by (McCabe, Smith et al. 2005):

$$Re = \frac{D\bar{V}\rho}{\mu} \quad 2-10$$

Where: D = diameter of the pipe

\bar{V} = average velocity of the fluid

ρ = density of fluid

μ = viscosity of fluid

When a fluid flows through a pipe the pressure loss can be calculated from the Darcys-Weisbach equation:

$$\Delta p = f \frac{L}{D} \frac{\rho V^2}{2} \quad 2-11$$

Where the pressure loss due to friction is a function of the ratio of the length to the diameter of the pipe, L/D , the density of the fluid ρ , the mean velocity of the flow, V , and the dimensionless coefficient of laminar or turbulent flow, f .

2.3.5 Effect of roughness on heat transfer

When a fluid flows through a pipe the roughness can create fluctuations in the flow. (McCabe, Harriott et al. 2005) states that the effect of roughness on heat transfer is of minor importance and is neglected in practical use. The heat transfer coefficient is greater for a rough surface than for a smooth surface in a turbulent flow with equal Reynolds numbers, but the effect is less than of the fluid friction.

Investigations performed by (Ceylan and Kelbaliyev 2003) have shown that for fully developed turbulent flow the roughness actually has an influence on the heat transfer. They showed by simplified equations that the convective heat transfer is influenced by the roughness of the tube wall. A rough surface causes turbulence which can break through the boundary layer and increase the contact area between the fluid and the cold wall. Consequently the heat transfer also increases.

2.3.6 Ignition by a jet of hot combustion products

The purpose of a flameproof enclosure is to prevent hot combustion products igniting an explosive atmosphere outside the chamber. For this to happen, the flame inside the enclosure has to be quenched and the hot jet has to lose its energy and temperature so it does not ignite the external explosive atmosphere. The cooling of the hot jet of combustion products happens inside the flame gap and when the jet mixes with cold unburned gas in the external chamber.

The classical thermal explosion theory formulated by (Frank-Kamenetskii 1955) describes the basic mechanisms for ignition. The main principal of this theory is that heat generation (\dot{Q}_G) has to exceed the heat loss (\dot{Q}_L) to get an ignition. Heat production happens due to chemical reactions and heat loss to the surroundings by conduction. The temperature-time history of an explosive mixture can, according to (Lee 2009), be described by :

$$\frac{dT}{dt} = \dot{Q}_G - \dot{Q}_L \quad 2-12$$

Figure 2-13 shows a small fixed volume, V_c , in the external chamber occupied with explosive gas. The hot combustion penetrates through the gap opening, and heats up the fixed volume.

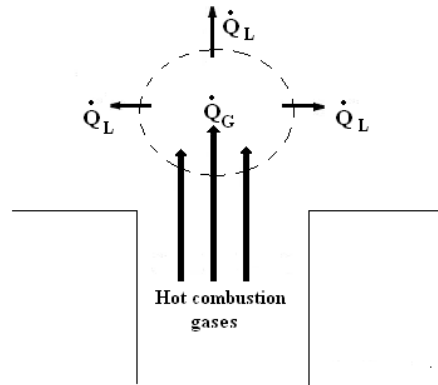


Figure 2-13 A fixed volume (V_c) in the external chamber, where it occurs heat generation (\dot{Q}_G) due to chemical reactions and heat loss (\dot{Q}_L) due to conduction. From (Solheim 2010).

Assuming that the volume does not expand and the temperature is uniform inside the small volume, Figure 2-14 illustrates heat generation (\dot{Q}_G) and heat loss (\dot{Q}_L) with temperature (T).

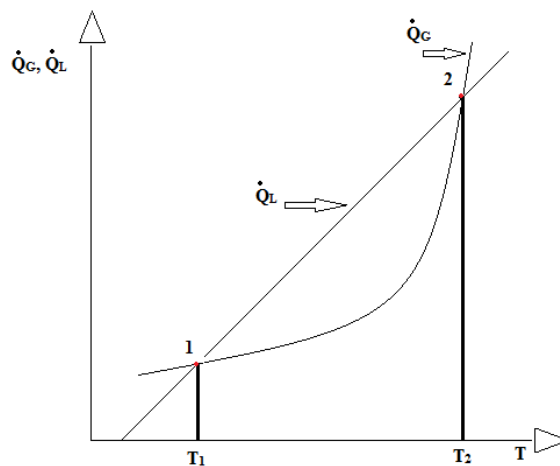


Figure 2-14 Ignition curve, heat loss by conduction (\dot{Q}_G) and heat production (\dot{Q}_L) as a function of temperature (T) in the reaction zone. Based on (Lee 2009).

The temperature in the fixed volume must be equal to T_2 or higher to get a re-ignition. Hence the heat generation exceeds the heat loss. When an ignition takes place a self-sustained combustion occurs of the surrounding gas mixture.

This is a simplified model of an ignition. In reality one cannot assume the volume to be constant, because when heat is applied to a system, the molecules will start moving faster and consequently the volume increases. In addition, heat is only supplied from one side and a uniform temperature is not the case in real reactions.

2.3.7 Cooling from entrainment and mixing with cold unburned gas in the external chamber

When hot combustion products penetrate through a narrow channel, a jet is formed. Because of the high pressure, the jet becomes turbulent and will mix with the ambient cold unburned gas. Figure 2-15 shows a plane turbulent jet. It can be divided into three regions:

- The core region: The velocity, temperature and concentration are constant. The hot combustion products mix with the cool unburned gas.
- Transition region: Turbulence is developed and the rate of cooling and mixing increases.
- Fully developed turbulent jet: The interaction between the hot and cold gas is at its maximum. Hence the cooling is at its maximum.

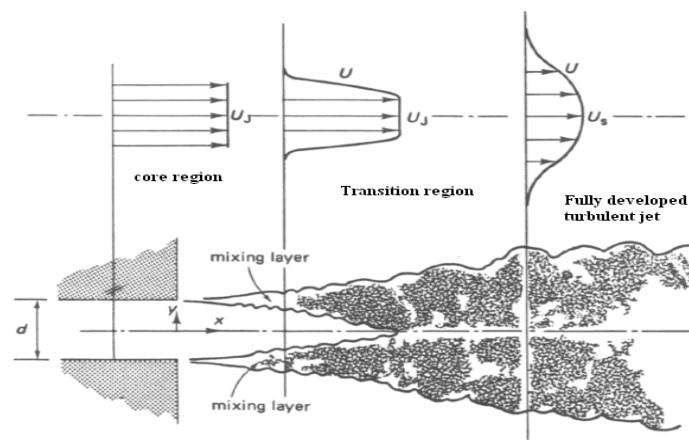


Figure 2-15 Illustration of a plane turbulent jet. The jet becomes self-preserving some distances after the two mixing layers near the wall exit have merged. From (Tennekes and Lumley 1972).

If the jet achieves favorable conditions and sufficient energy in one of the three regions, a re-ignition in the surrounding unburned gas will occur. In the core region the velocity of the jet is often too high to give sufficient contact time between the hot jet and the cold unburned gas. As the velocity decreases in the transition region, the contact time increases. Heat generation versus heat loss determines if a re-ignition can take place, see Figure 2-14.

2.4 Previous experimental research on explosion transmission through narrow gaps

2.4.1 H. Phillips work

Harry Phillips did a thoroughly work on the physical mechanism of flameproof enclosures, and related a set of equations to his experimental work. Only an excerpt of his extensive work on explosion transmission trough narrow gaps is presented in this section.

Phillips recorded hot combustions products out of an orifice with a Schlieren system to indicate the way in which the external mixture is ignited. Figure 2-16 shows the photograph of an ignition probability of 0.5. The flame developed as a ball of fire at the head of the advancing jet of hot gas ejected from the gap, and appeared first 50 mm away from the orifice. When the gaps were larger the ignition appeared closer to the orifice, and further away for smaller gaps until a stage was reached where no ignition was obtained.

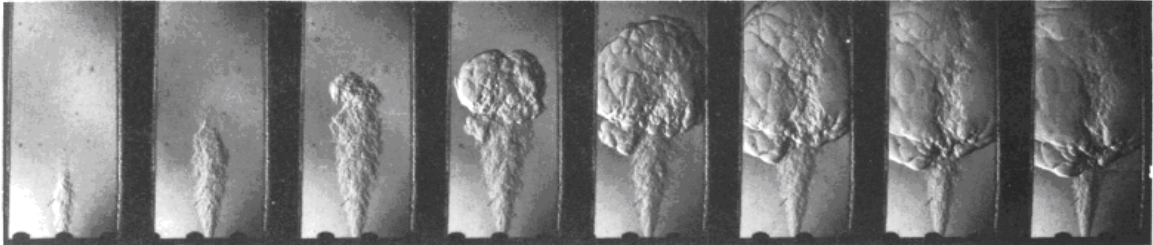


Figure 2-16 Schlieren photographs of 50 per cent probability for re-ignition. From (Phillips 1972)

Phillips did a numerical analysis of the temperature of the vortex head to decide whether the jet could ignite the gas in the secondary chamber. When the temperature dropped in the vortex head due to entrainment and mixing with the cold unburned gas, no ignition was observed. Increases in the temperature of the vortex above the ignition temperature for the gas lead to an ignition. In other words, the rate of heat production from the combustion process exceeded the rate of heat loss due to mixing with the cold unburned gas.

Ignition can be considered as the result of mixing and combustion within the hot jet. Phillips did an energy balance over a small volume of the vortex to find an expression for the rate of combustion, ω :

$$\omega = \frac{1}{\eta_c} \cdot \frac{d\eta}{dt} + \frac{1}{m} \cdot \frac{dm}{dt} \tag{2-13}$$

Where:

m = mass of gas in the vortex

η_c = combustion efficiency

The combustion efficiency can be expressed as:

$$\eta_c = \frac{T - T_u}{T_m - T_u} \quad 2-14$$

Where:

T = jet temperature

T_u = ambient temperature

T_m = maximum flame temperature.

The function $\frac{1}{m} \cdot \frac{dm}{dt} = \frac{z}{t}$, is the rate of entrainment into the jet. The factor z is an experimental determined entrainment factor for jets. A high value for z indicates that the velocity of the jet increases with time.

The temperature change with time is shown in Figure 2-17. The lowermost line represents a pure mixing process with no combustion where the heat loss exceeds the heat generation. The three upper lines are all ignitions. At first the temperature drops, but the heat generation exceeds the heat loss due to entrainment, and the temperature rises to maximum flame temperature and ignites the gas. The three lines in the middle are failures to ignite. They have a higher temperature than the pure mixing line and represent a zone of burning close to the gap while the jet is still hot. Further mixing decreases the temperature and extinguishes the flame. This explains the flash that has been observed in experiments without a general ignition.

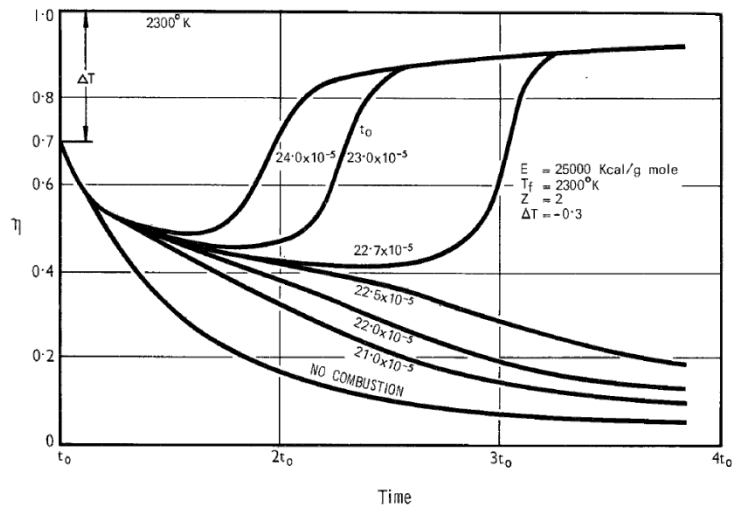


Figure 2-17 Analogue computer curves of vortex temperature. η is a non-dimensional temperature (combustion efficiency) and t_0 denotes the starting time in seconds from a point source until the vortex fills the orifice. From (Phillips 1972).

The effect of initial pressure

Phillips showed that if the pressure increases, the heat transfer is reduced and the reaction rate increases. The net effect of increased pressure is to reduce the critical gap (Phillips, 1973).

Phillips found a critical ignition point where the external mixture is most likely to occur. At this point the pressure and velocity was low, so he used heat transfer calculations for laminar flow. Figure 2-18 shows the variation of safe gaps due to pressure, and are based on Phillips calculations. For low pressures, an increase in the pressure leads to a decrease in the safe gap. Because of the low pressure and velocity, the cooling by entrainment and mixing with the cold unburned gas is low, and the safe gap reaches its minimum at approximately 1.5 bar. When the pressure is further increased the safe increases. The rate of cooling exceed the heat generation by the combustion process. The safe gap reaches its maximum at approximately 2.5 bar and any further increase in the pressure decrease the safe gap. The pressure in the apparatus Phillips used for his experiments could not exceed the pressure at the break point, and the safe gap is at its minimum. (Phillips 1988)

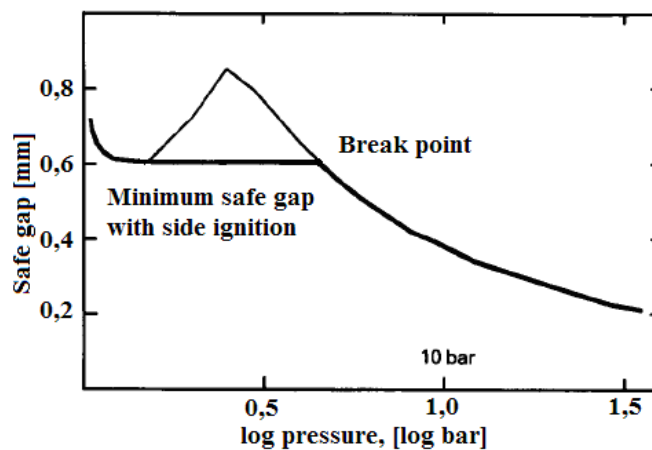


Figure 2-18 The 's' curve showing a minimum in safe gap at 1.5 bar and a break point at 4.6 bar. From (Phillips 1988).

2.4.2 T. Redeker

(Redeker 1981) studied the effect of different parameters on the MESG and the safety of flame proof equipment. Only the parameters relevant for this present thesis are presented.

Influence of the location of the ignition source

Redeker found that the influence of the ignition source location is much greater for larger inner volumes ($>20 \text{ cm}^3$) than for small inner volumes. From Figure 2-19, Redeker also stated that the effect of ignition position increased with decreasing flame velocity. Methane has the lowest flame velocity of the gases represented in Figure 2-19.

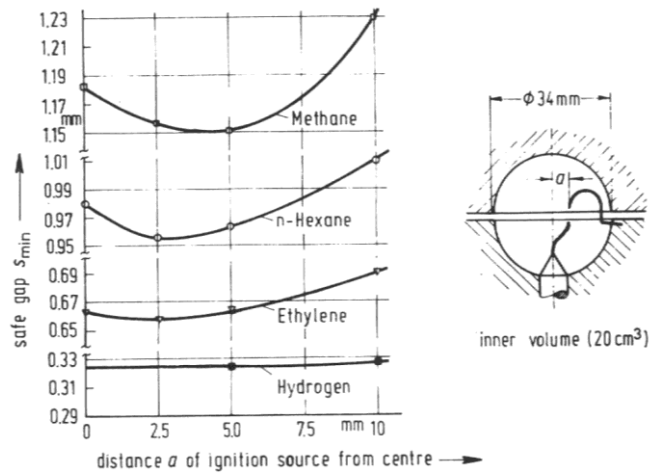


Figure 2-19 Safe gap s_{min} for the most incendive gas/air and vapor/air mixture as a function of location of ignition source, determined in the test apparatus with an inner volume of 20 cm^3 and gap length of 25 mm. From (Redeker 1981)

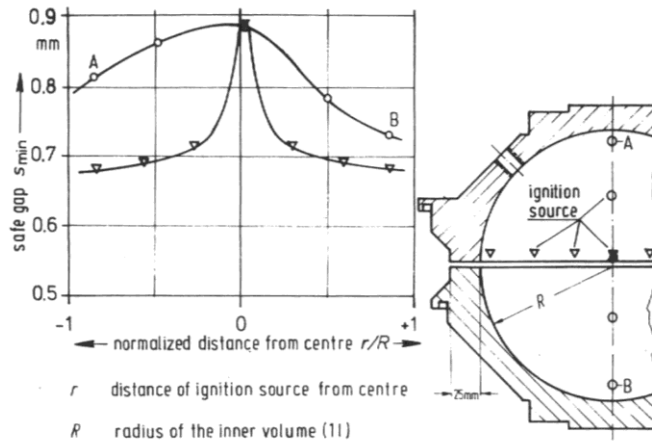


Figure 2-20 Safe gap s_{min} of most incendive Ethylene/air mixture as a function of location of ignition source, determined in a test apparatus with an inner volume of 1 l and a gap length of 25 mm. From (Redeker 1981)

Redeker suggested that the results presented in Figure 2-20 showed how the transition from laminar to turbulent flow was brought about by shifting the ignition source location in the gap plane from the gap edge towards the middle.

Influence of concentration

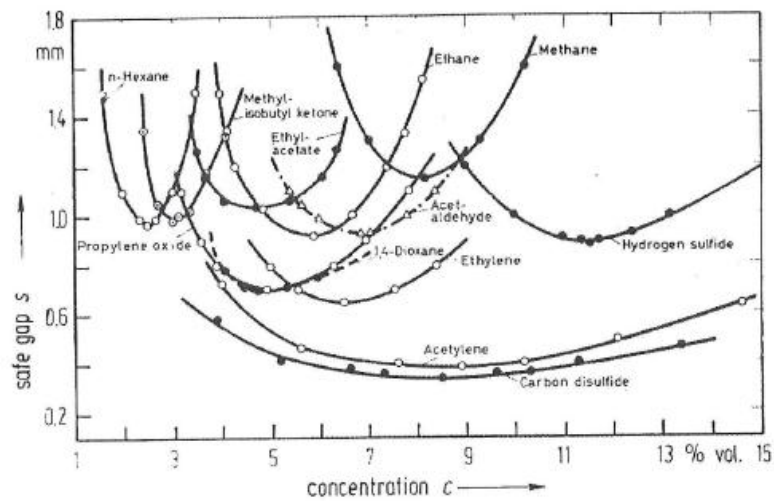


Figure 2-21 Safe gap s as a function of the concentration c of combustible gas or vapour in mixture with air, determined in the 20 cm^3 standard safe gap test apparatus. From (Redeker 1981)

Redeker found that at the most incendive mixture of gas/air the safe gap is at its minimum. For highly reactive substances the safe gap slightly varies over a wide concentration range, as seen for acetylene and carbon disulfide in Figure 2-21.

2.4.3 Ø. Larsen

(Larsen 1998) did experiments to find critical hole diameters for explosion transmission from a primary chamber into an ambient gas. Some of his experiments performed in a 1 liter primary chamber relevant for this thesis are presented.

Larsen investigated the optimal propane concentration in air for flame transmission into the secondary chamber. The experiments gave a U-shaped curve, shown in Figure 2-22. The curve has no distinct minimum, but a constant level of minimum hole diameters for flame transmission over a wide propane concentration range from 3 to 6 vol. %.(Larsen and Eckhoff 2000)

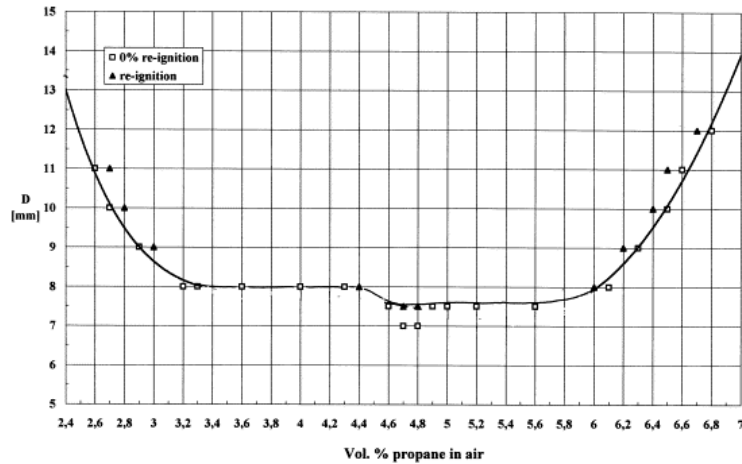


Figure 2-22 Results from experiments with a cylindrical 1-l primary chamber. Distance X_i from the electrical spark ignition source to the entrance of the cylindrical flame transmission hole is 94 mm. D is the hole diameter and the hole length is 12.5 mm. From (Larsen 1998).

Maximum explosion pressure as a function of the concentration is shown in Figure 2-23. The highest maximum explosion pressure was obtained at a concentration of 4.6 vol. % propane in air, which is above the stoichiometric value of 4.02 vol. %.

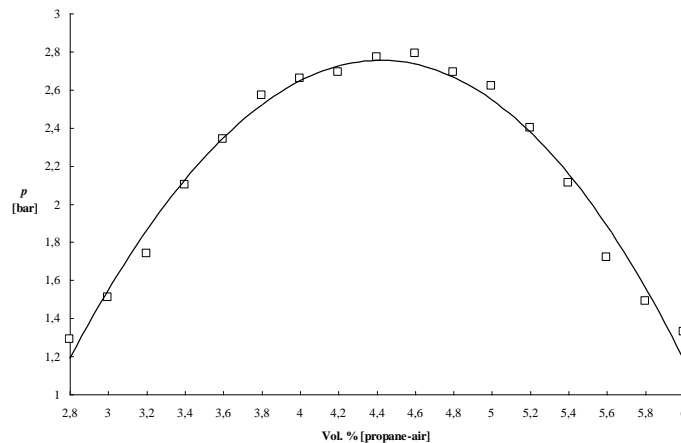


Figure 2-23 Max explosion pressure as a function of concentration. Hole diameter $D = 9,5$ mm, volume of primary chamber $V = 1$ -l and ignition distance $X_i = 94$ mm i.e. closed to the bottom end.(Larsen 1998)

Larsen also did experiments to find the ignition position in the primary chamber which gave the smallest hole diameter. His results for the experiments performed in the 1-l chamber are presented in Figure 2-24.

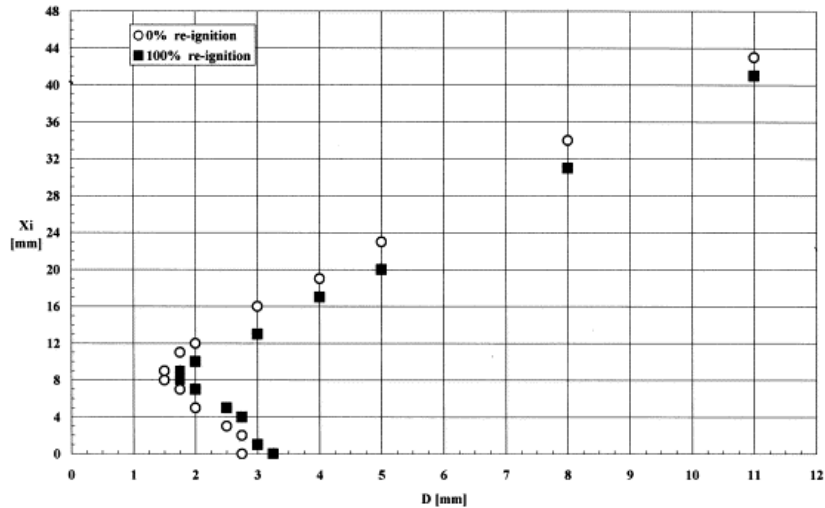


Figure 2-24 Safe diameter D_S and D_{10} for various ignition-distances X_i . Primary volume $V = 1\text{-l}$ and 4,2-vol. % propane-air. From (Larsen 1998).

D_S is the diameter giving no re-ignitions in ten subsequent experiments and D_{10} is the diameter giving ten subsequent re-ignitions. The hole diameter was varied together with ignition distance. The critical hole diameter occurred a small finite distance away from the hole entrance. The critical hole diameter increased systematically when the ignition point got very close to the hole entrance. The results indicate that the minimum tube diameter for re-ignition is about half the minimum diameter for laminar flame propagation. This is in good agreement with the rule-of-thumb that the MESG of a premixed gas is about half its laminar quenching distance. (Larsen and Eckhoff 2000)

Figure 2-25 shows how the pressure increased with increasing distance from the hole entrance. (Solheim 2010) discussed an increasing pressure with increasing ignition distance in his master thesis. See section 2.4.6.

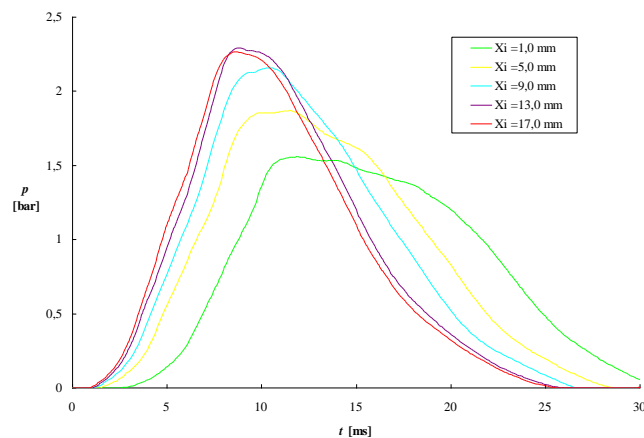


Figure 2-25 Explosion pressure as a function of time for various ignition distances. Hole diameter $D = 2,0$ mm, primary volume $V = 21\text{-ml}$ and 4,2-vol. % propane-air concentrations. From (Larsen 1998).

2.4.4 H.E.Z. Opsvik

(Opsvik 2010) performed experimental investigations in the self-constructed Plane Circular Flange Apparatus (PCFA) and determined the MESH value for undamaged, sandblasted and rusted flanges. Experiments on rusted flanges with greater average roughness than the IEC requirements of $6.3\mu\text{m}$ gave a larger MESH value than the undamaged flange. The flanges were rusted separately and screwed together prior to the explosion test. The sandblasted flanges gave reduction in the MESH value. He explained that this could be a result of increased gap opening rather than an effect from roughness on the flow through the gap.

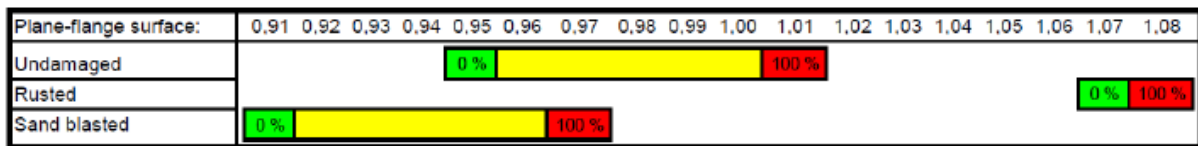


Figure 2-26 Explosion experiments with variation of circular flange openings. No re-ignition is indicated with green color, while 100 % re-ignition is red. The transition range is the yellow bar. From (Opsvik 2010).

2.4.5 A. Grov

(Grov 2010) continued the work of (Opsvik 2010) in the PCFA, in addition he did experiments in the Plane Rectangular Slit Apparatus (PRSA) which is the same apparatus used in this present experimental work. He found that experiments performed in the PCFA and the PRSA was in good correlation even though the apparatus is different. Propane was used as the test gas throughout all his work. Only an excerpt of his experiments is presented.

As (Larsen 1998) did, Grov also investigated the ignition point most favorable for re-ignition in the secondary chamber. Larsen had operated with cylindrical holes, while Grov investigated rectangular flanges. Grov found the most favorable ignition position to be 14 mm from gap opening, and the MESH for propane in the PRSA to be 0.98 mm. Figure 2-27 shows the results. Compared to the experiments (Larsen 1998) did, the shape of the curve is quite similar.

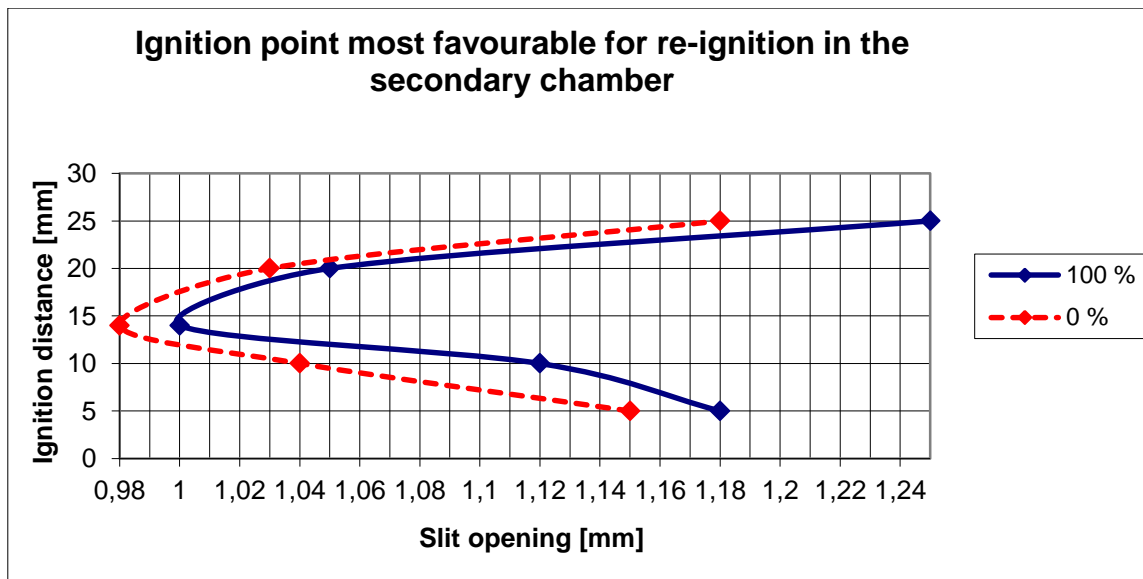


Figure 2-27 Determination of the ignition position most favorable for re-ignition in the secondary chamber in the Plane Rectangular Slit Apparatus with 4.2 vol. % propane in air and undamaged slit. The solid line is the gap opening giving re-ignition for ten experiments for the given ignition position, the dotted line is the gap opening giving no re-ignition for ten experiments for the given ignition position. From (Grovs 2010).

Rusted flame gap surfaces

Grovs investigated the influence of rust on two flame gaps in the PRSA. He placed the slits separately in the sea, and attached the slits together before performing the experiments. The experiments showed a reduction of 15 % of the MESG value compared to an undamaged slit. He assumed the difference from his results to the ones obtained by (Opsvik 2010) were because of compression of porous iron oxide. The torque Opsvik used to mount the flanges together in the PCFA was higher than the torque Grovs used in the PRSA. Grovs explained that this would lead to that the actual value of the gap opening was smaller than the value reported by (Opsvik 2010).

Fabricated damages on the flame gap surface

Grovs did experiments with multiple crosswise grooves of 2 mm width and 3 mm depth in the PCFA and the PRSA. The results showed that crosswise grooves in relation to the flow in the flame gap had a better ability to prevent re-ignition in the secondary chamber compared to the undamaged flame gap. The slit tested in the PRSA gave an increase in the MESG value of 12.2 % and the slit tested in the PCFA gave an increase of 20 % in the MESG, compared to the undamaged gap surfaces. He assumed that reason for the increase in the MESG is because when the unburned gas in the primary chamber is pushed through the flame gap, the grooves will create fluctuations and turbulence of the unburned gas into the external chamber. So in the arrival of the first jet of hot combustion products in the external chamber, there will already be a turbulent state. This would again lead to a more efficient cooling of the hot combustion products by entrainment and mixing with cold unburned gas. He also observed a significant increase in the pressure build up with the crosswise grooves. He explained that this would indicate more resistance on the flowing gases through the gap, and that the pressure is larger before the gases are ejected through the gap and into the external chamber.

Multiple lengthwise grooves were also tested by Grov in the PRSA and the modified PCFA. Similar to the slits with the crosswise grooves, the lengthwise grooves showed a better ability to prevent re-ignition in the secondary chamber than the undamaged gap. However he had a hard time explaining the reason for this, because from pressure measurements he observed that the lengthwise grooves increased the ventilation area and therefore the velocity of the combustion decreased. He explained that the cooling in the gap only was of second order importance so the reason was probably because of the turbulence created by the lengthwise grooves.

2.4.6 F. Solheim

(Solheim 2010) continued the work done by (Opsvik 2010) and (Grov 2010). Some of his work on dust was performed in the Plane Circular Flange Apparatus (PCFA) but most of his work was carried out in the PRSA. Some of his work in the PRSA is presented in this section.

Rusted flame gap surfaces

Solheim placed five attached slit sets with undamaged flame gap surface at the sea side for rusting. To get a more realistic corrosion on the slits, they were attached before rusting and not rusted separately as (Opsvik 2010) and (Grov 2010) did before him. Experiments done on the slits after the rusting period gave no re-ignition on any of the slit sets, even though the slit with the largest gap opening of 1.01 mm gave 100% re-ignition in undamaged state. Solheim observed that a noticeable quantity of rust was blown of the gap surface by the first explosion. He also noticed a decrease in the maximum pressure for the ten subsequent explosions tests performed on each of the five slit sets. He explained this by when rust leaves the gap surface, the effective venting area increases. In all of the experiments for the five slits except one, the mean pressure increased after the slits had rusted. Solheim explained that the venting had become smaller and the corroded configuration had not been totally blown out after ten explosions. The rusted configuration also lead to a higher resistance in the gap and caused a higher initial pressure. Sparks were observed in the secondary chamber during the first explosion on each set. The sparks did not ignite the explosive gas mixture. He assumed that the sparks were porous iron atoms that combust.

Experiments to find the most favorable ignition position for re-ignition in the secondary chamber with multiple crosswise grooves

Solheim did experiments to find out if the ignition position for undamaged flame gaps was valid for slits with crosswise grooves. He used the same procedure as Grov did for undamaged slits. Figure 2-28 shows the results.

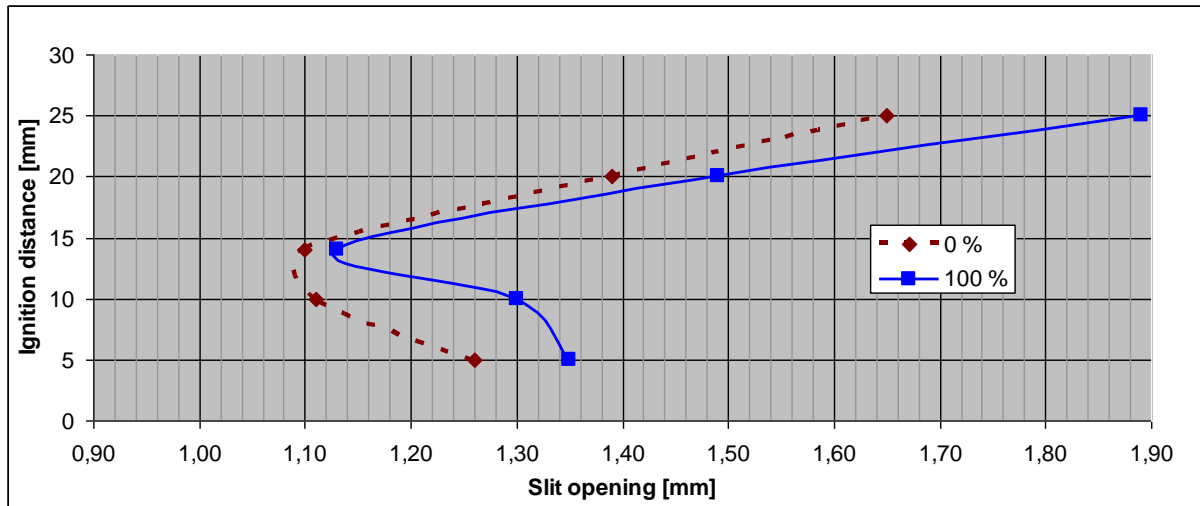


Figure 2-28 The most favorable ignition point for re-ignition in the secondary chamber in experiments with multiple crosswise grooves (PH-7.2.3) in the gap surface. The red dotted line represents the largest gap opening that gave no re-ignition in the secondary chamber after ten subsequent experiments, whereas the blue line represents the smallest gap opening that gave 100 % re-ignition in ten subsequent experiments. All experiments were performed with 4.2 vol. % propane in air. (Solheim 2010)

His experiments showed that an ignition position of 14 mm from the flame gap entrance also was the most favorable ignition position for slits with multiple crosswise grooves. The pressure in the primary chamber increased with increasing distance from the safe gap. The results correlated well with the results (Larsen 1998) obtained, and Solheim suggested that this implied that the same physical mechanism is applicable in relation to pressure build up for an explosion vented through a slit surface with crosswise grooves.

He explained that the increase in ignition distance and pressure would lead to an increase of the flow through the gap. When the primary chamber is emptied faster, the time for cooling of the hot combustion gases inside the chamber and the slit gets shorter. A larger amount of the hot combustion gases will then reach the explosive gas in the external chamber within a limited time. But as the velocity is increased, the turbulence build-up above the gap opening would also increase, and the energy that possibly ignited the external gas would be dispersed over a larger area above the gap opening, and the probability for re-ignition decreased. He therefore stated that at the ignition position of 14 mm the interaction between the pressure, velocity and turbulence level through the slits favors a re-ignition of the explosive mixture in the external chamber.

Experiments performed with different depths on the perforating crosswise grooves

Solheim used four slit sets with seven crosswise grooves of varying depth. The previous work of Grov had shown that the gap efficiency and the MESG value increased after milling the grooves into an undamaged gap surface. Solheim wanted to investigate if there were other configurations that improved the gap efficiency even more. His result was that the slit set with the deepest crosswise grooves had the highest MESG value, but there was no clear correlation between the depth and MESG value for the four slit sets. The mean pressures for the four slit sets were also recorded. The pressure increased with increasing depth of the crosswise grooves.

In Solheim's discussion of the results he explains that an increase in the relative roughness leads to a greater friction factor. This again leads to a decrease in the velocity of the penetrating combustions gases. A decrease in the flux of hot combustion products from the primary chamber, leads to a greater pressure drop inside the channel and a greater maximum pressure in the primary chamber. He also explains the general improvement of the gap to be because of increased heat transfer to the gap wall. Literature has shown that an increase in the roughness leads to greater heat transfer because of the developed turbulence and then an increased fluid to solid contact area. Temperature measurements supported his conclusion about the heat transfer. The temperature decreased with 50 % when replacing the undamaged slit with a slit with crosswise grooves.

Experiments performed with slits with different width on the perforating crosswise grooves

Solheim did experiments on two sets with different width on the crosswise grooves. From his experiments he found that the width of the crosswise grooves is of great importance to the gap efficiency. The larger the width the better is the efficiency. The MESG value for the slit with grooves of 1 mm width, increased by 12 % compared to the undamaged slit. A width of 2 mm increased with 34 % in the MESG value. He found that the pressure increased with increased width size, and explained the reason for this is the same as for the crosswise grooves with different depth.

High speed camera recordings- comparison of slit with multiple crosswise grooves and undamaged slit

Solheim shot several experiments with a high speed camera to investigate if there were any difference in the re-ignition process for undamaged gap surface and multiple crosswise grooves. The results showed that the ignition in the secondary chamber with an undamaged slit occurred as a detached sphere approximately one centimeter above the gap opening. The re-ignition for the slit with crosswise grooves occurred at a lower altitude than for the undamaged slit and it looked like a jet penetrating out from the flame gap.

2.5 Basic corrosion theory

Corrosion is defined according to (Bardal 2004) as “an attack on a metallic material by reaction with its environment”. Formation of rust is a great problem in the offshore industry because of the presence of salt water. Dissolved salt increases the conductivity of the aqueous solution formed of the metal and increase the rate of electrochemical corrosion. Exposed enclosures are often made of carbon steel, which consist of iron. The formation of rust from iron is therefor used in the following example.

A corrosion process consists of an anodic and a cathodic reaction. In the anodic reaction (oxidation) the metal, in this example iron (Fe), is dissolved and transferred to the solution as ions Fe^{2+} . The cathodic reaction is the reduction of oxygen. The process makes an electrical circuit without any accumulation of charges. Electrons released by the anodic reaction are conducted through the metal to the cathodic area where they are consumed in the cathodic reaction. The iron ions Fe^{2+} are conducted towards the OH^- ions, and together they form iron(II)hydroxide $Fe(OH)_2$. Iron(II)hydroxide is not stable, and with the access of oxygen and water it oxidizes to iron(III)hydroxide, $Fe(OH)_3$. Iron(III)hydroxide may also be expressed as $FeOOH + H_2O$. $FeOOH$ is the ordinary red/brown rust. Figure 2-29 shows how the corrosion process eats up the solid surface and causes elevations of rust formation.

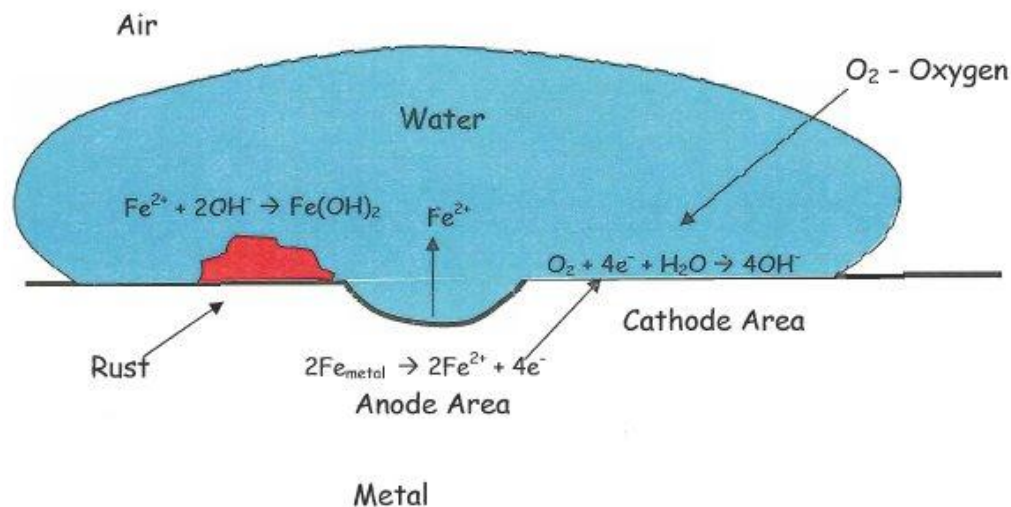


Figure 2-29 Illustration of wet corrosion.

Offshore platforms are typically placed between the splash zone and the marine atmosphere. Figure 2-30 illustrates the different areas with the corresponding corrosion rates. The corrosion rate depends on the supply of oxygen, and will be highest in the splash zone where a thin film exists a major part of the time. The parts of the corrosion layer are frequently washed away which leads to an increase in the corrosion rate. Average corrosion rate on steel in seawater is 0.1-0.15mm/year.

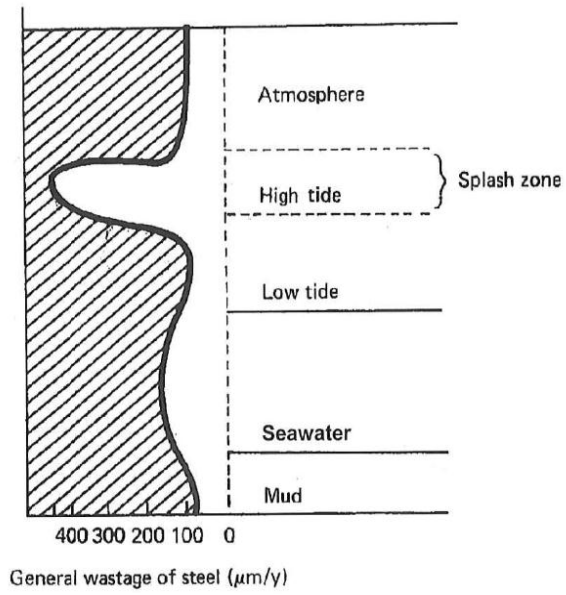


Figure 2-30 Corrosion rate on steel in seawater as a function of depth. (Depth vs $\mu\text{m}/\text{year}$). From (Bardal 2004).

2.6 Ethylene

Ethylene is a colorless gas with a characteristic sweet odor. The gas is not poisonous but at high concentrations it can act narcotic and if the air is displaced there is a risk of choking.

Ethylene is the simplest of the alkenes (olefins), classified as an unsaturated hydrocarbon because of its carbon-carbon double bond. It is the most important organic chemical, in terms of quantity produced. It is the feedstock in the manufacture of PVC and polyethylene. Together with air ethylene forms an explosive atmosphere. It is classified as group IIB gas and is highly reactive. For a stoichiometric combustion in air the concentration of ethylene is 6,52 vol. %. Appendix B-1 shows the calculation for a stoichiometric combustion of ethylene in air. Table 2-7 lists some of the physical properties of ethylene.

Table 2-7 Physical properties of ethylene. Based on (Eckhoff 2005; AS 2007)

Gas	Ethylene
Chemical formula	C ₂ H ₄
Critical temperature [°C]	9,9
Critical pressure [bar]	51,2
Boiling point [°C]	-103,7
Density, kg/m ³ (0°C, 1 atm)	1,26
Lower flammable limit [vol.% in air]	2,7
Upper flammable limit [vol.% in air]	36
Minimum ignition temperature [°C]	425
MESG [mm]	0,65
Adiabatic flame temperature (constant volume) [K]	2740
Temperature class	T2
Gas group	IIB

3 Experimental Procedures and Apparatus

3.1 Overall experimental approach

The experiments in this work are performed in an apparatus called the Plane Rectangular Slit Apparatus, (PRSA). The apparatus is referred to as the PRSA throughout this work.

The PRSA was built by (Larsen 1998) and professor Eckhoff, and was also used by (Einarsen 2001), (Grosv 2010) and (Solheim 2010) in their experimental thesis. The apparatus has been modified since it was first built. This makes it a reliable and efficient tool for experiments with safe gaps. The experimental procedure is described in Appendix A.

The main approach is to observe if a re-ignition occurs in the secondary chamber. Slits with different surface configuration are replaced and the MESG is chosen to be a parameter for deciding the ability of the flame gap to prevent a re-ignition in the secondary chamber. The ability to prevent a flame transmission is denoted as the gap efficiency further in this thesis. Ethylene was used as the test gas throughout all experiments.

The term “safe gape” is used for the largest gap opening which gave no re-ignitions in ten subsequent experiments under other conditions than the “worst case” scenario. In example when the ignition source is not placed at the most dangerous position.

3.2 The Plane Rectangular Slit Apparatus

The PRSA consist of a primary chamber of 1 liter and an external chamber of 3 liters. The two chambers are connected via a rectangular flame gap, which is replaceable with different flame gap surfaces. The gas is ignited in the primary chamber by an electrical spark. The ignition source can be vertically adjusted from the flame gap. The explosion is vented trough the slit opening and into external chamber.

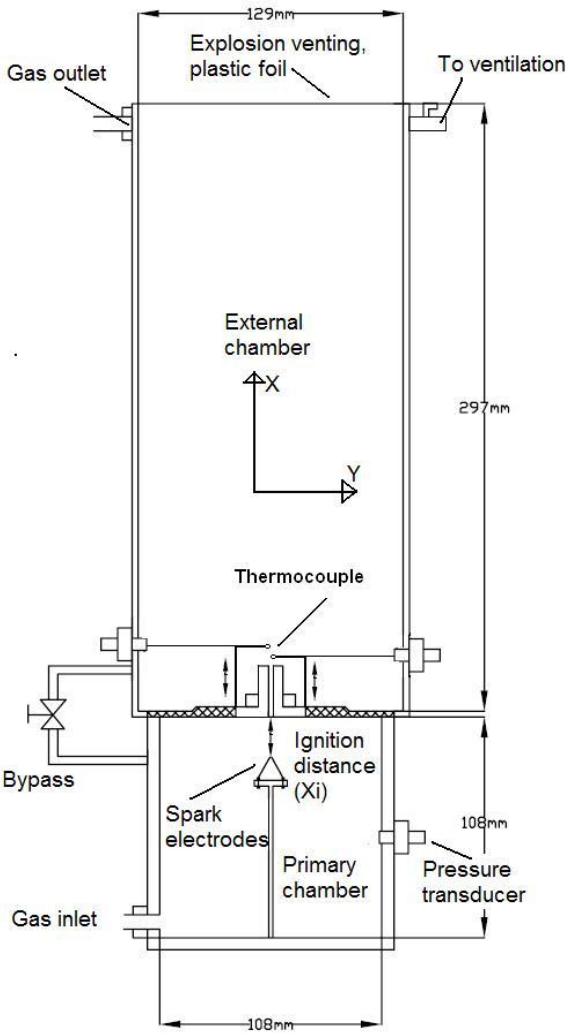


Figure 3-1 A cross section of the Plane Rectangular Slit Apparatus. Consist of 1 liter primary chamber, a plane flame gap with 25 mm width to a secondary chamber of 3 liters. The plane flame gap is used for determining MESG for different surfaces in ethylene/air mixture. From (Solheim 2010).

Table 3-1 Specification of the Plane Rectangular Slit Apparatus (PRSA). From (Solheim 2010)

Specifications of the PRSA	
Volume primary chamber	1000 cm
Volume, secondary chamber	3000 cm
Slit width	25 mm
Slit length	56 mm
Distance "shims"	Varying distance
Ignition source	Spark electrodes, located in the primary chamber
Thermocouples	Adjustable in the secondary chamber
Pressure gauge	Located in the primary chamber

3.2.1 Slits

Two slits creating a flame gap is shown in Figure 3-2. The distance pieces used in the flame gap were industrial “shims” to get a constant gap opening between the slits. The slits were fastened with a low torque of 20cNm at the upper and lower part of the slit to get a uniform pressure and a constant gap opening. This method to insure a constant gap opening is a modification made by (Grosv 2010) and (Opsvik 2010). A more detailed description of the fastening method is described in Appendix A-2.1.

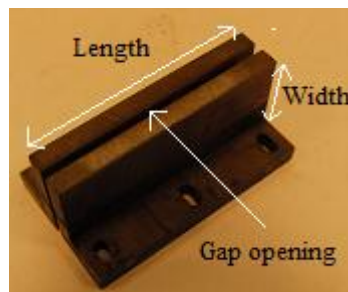


Figure 3-2 Photography that illustrates the slit width, the slit length and the gap opening.



Figure 3-3 Distance pieces

Slits with seven crosswise grooves

A slit set with seven crosswise grooves is shown in Figure 3-4. This slit was originally made for the work performed by (Grosv 2010). Slits with different width and depth of the grooves were made for the work performed by (Solheim 2010).



Figure 3-4 Slits with crosswise grooves. Surface configuration PH-7.2.3.

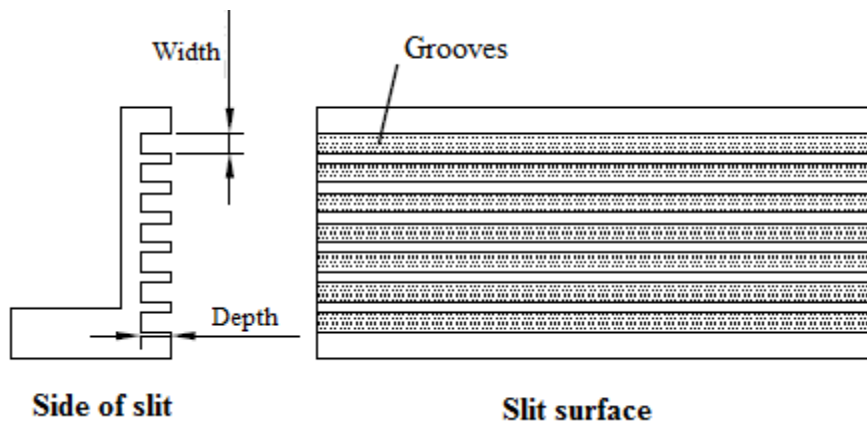


Figure 3-5 Illustration of the dimensions of the slit with seven crosswise grooves. Based on (Grosv 2010)

Grosv created a name system which distinguishes between the slit sets with different surface configurations. Figure 3-6 is an illustration of the naming system. He distinguished between grooves that go in the same direction (lengthwise) and opposite direction (crosswise) as the flow through the flame gap, see Figure 3-8. In this work, slits with crosswise grooves of different depth were investigated. Table 3-2 gives the specification of the four slit sets.

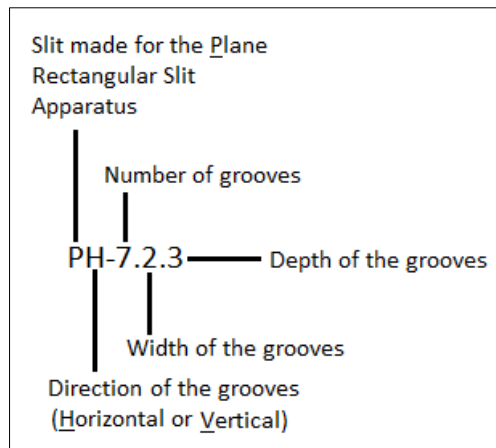


Figure 3-6 Illustration of the name system for different slit configurations. From (Solheim 2010).

Table 3-2 Specifications of four different slit sets with different depth. From (Solheim 2010)

Specifications	PH-7.2.3	PH-7.2.2	PH-7.2.1	PH-7.2.0,5
Material	Carbon steel	Carbon steel	Carbon steel	Carbon steel
Rz [μm]	2,0	2,0	2,0	2,0
Ra [μm]	0,2	0,2	0,2	0,2
Length of slit [mm]	25	25	25	25
Width of slit [mm]	56,3	56,3	56,3	56,3
Thickness of slit [mm]	5,0	5,0	5,0	5,0
Number of grooves	7	7	7	7
Width of grooves [mm]	2,0	2,0	2,0	2,0
Depth of grooves [mm]	3,0	2,0	1,0	0,5
Heat capacity [$\text{J/g}\cdot\text{C}^\circ$]	0,452	0,452	0,452	0,452
Thermal conductivity [W/mK]	45	45	45	45

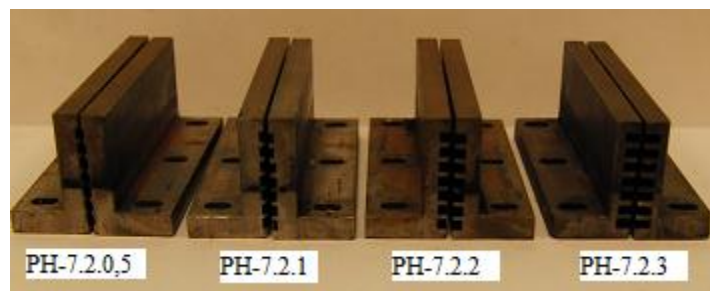


Figure 3-7 Four slit sets with different depth of the grooves.

3.2.2 Direction of the flow in the primary chamber

When the gas in the primary is ignited, it will lead to a growing spherical flame which will be quenched in the gap opening. Hot combustion products will then be pushed through the gap opening, due to the pressure rise in the primary chamber, and a jet of hot combustion products will enter the secondary chamber. The flow direction is illustrated in Figure 3-8.

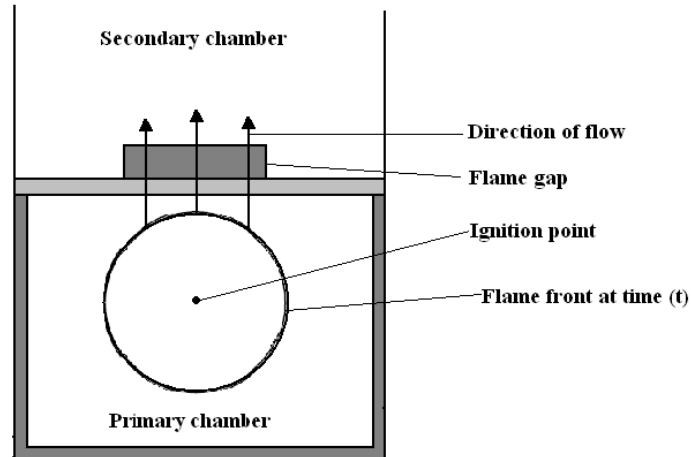


Figure 3-8 Illustration of which direction the venting of the hot combustion gases will appear in the PRSA. The flame front develops as a sphere from the ignition point. From (Solheim 2010).

3.2.3 Adjustment of the ignition position

The ignition source in the primary chamber consists of two spark electrodes, see Figure 3-9. It can be adjusted vertically from the gap opening and towards the bottom of the primary chamber. The optimal ignition position with ethylene/air mixture is a part of the experimental research in this thesis.



Figure 3-9 Photograph of the adjustable ignition source located in the primary chamber.

3.2.4 Adjustment of the thermocouple position

Solheim did some modifications on the PRSA to be able to measure the temperature above the flame gap in the secondary chamber. He mounted two steel “rods” on the plate that separates the primary chamber from the secondary chamber. The thermocouple wires were fastened with small clips on the steel “rods”, so each thermocouple was located a given distance vertically above the gap opening. Both of the steel “rods” is replaceable, so it is possible to adjust the distance from the gap opening by mounting a new “rod” with different length. (Solheim 2010)

The temperature is measured at one point only in this experimental work.

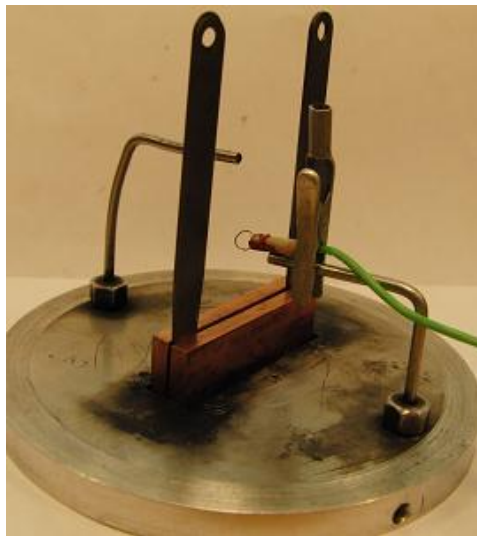


Figure 3-10 Photograph of the replaceable steel rods on which the thermocouples were “clips” on.

3.3 Different experiments carried out

3.3.1 Rusted gap surface

Six attached slits with undamaged flame gap surface were placed at the sea side for about one and a half month. The slits were placed midway between high and low tide. Ten experiments were conducted on each slit set, before and after rusting.

The ignition position was chosen on the basis of previous work in the PRSA. The gas concentration was chosen to be a stoichiometric concentration of ethylene in air which is, according to (IEC 2010), the most incentive mixture. The MESG value for ethylene in a standardized test apparatus is 0.65 mm. Some preliminary experiments were conducted to find the safe gap at the chosen ignition position for ethylene in the PRSA.

Table 3-3 Specifications of the undamaged slit sets and the rusted slit sets.

Specifications	Undamaged gap surface	Rusted gap surface
Material	Carbon steel	Carbon steel coated with rust
Rz [μm]	2,0	30*
Ra [μm]	0,2	7*
Length of slit [mm]	25	25
Width of slit [mm]	56,3	56,3
Thickness of slit [mm]	5	5*
Heat capacity [J/g-C°]	0,452	0,452*
Thermal conductivity	45	45*

*The thermal conductivity and the heat capacity may change due to formation of rust. The values of roughness of the rusted gap surface are estimated. The estimations of the roughness values is based on measurements performed by (Grosv 2010). The roughness Grosv measured was on slit which had been corroded separately. In this work the slits were attached prior to rusting. The gap opening was blocked by rust and the rust was assumed to be better attached between two surfaces close to each other than of rust on a single surface. This was taken into account when estimating the values of roughness.

Motivation

A common damage on equipment used in the offshore industry is corrosion. It is therefore of interest to investigate the effect of such damage on safety equipment in relation to explosion hazard.

Previous experiments have been carried out on the effect of rust by (Opsvik 2010), (Grosv 2010) and (Solheim 2010). Grosv's experiments gave a reduction in the MESG value of 15.3% in the PRSA, while Opsvik got results showing an increase in the MESG value of 12.6% in the Plane Circular Flange Apparatus. Solheim's experiments gave no re-ignitions on the rusted flame gaps. It is important to mention that the slits Solheim placed out for rusting were attached to each other, while Grosv and Opsvik placed the slits separately. To do a further investigation of the effect of rust a more reactive gas, ethylene, has been used.

Solheim observed sparks, which he assumed to be porous iron atoms that combusted, during the first explosion test on each rusted slit. Ethylene is a more reactive gas and it is interesting to see if such sparks causes a danger for a re-ignition in the secondary chamber. The first explosion tests on each rusted slit were therefor recorded with a high speed camera.

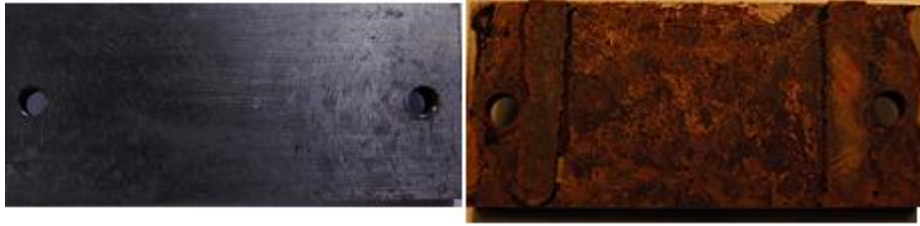


Figure 3-11 Undamaged gap surface and rusted gap surface after ten explosion tests.

3.3.2 The most dangerous concentration of ethylene for re-ignition in the secondary chamber

Several experiments with different concentrations under and above the stoichiometric concentration were performed to find the most dangerous concentration. The undamaged gap opening was held constant and the concentration giving most re-ignitions in ten subsequent experiments was determined to be the most dangerous concentration.

Motivation

The most incendive mixture is according to (IEC 2010) 6.5vol.% ethylene in air. The values presented in the standard are a result of experimental determination and will vary with different experimental apparatus and procedures. Since experiments with ethylene never have been performed in the PRSA, it is necessary to find the most dangerous concentration valid for this apparatus to make sure that further investigations in the PRSA is conducted under worst case conditions.

3.3.3 Optimal ignition position for re-ignition in the secondary chamber with undamaged slits and the MESG

The safe gap at different ignition positions was determined. The smallest safe gap was determined to be the MESG and the corresponding ignition distance to be the most favorable for a re-ignition in the secondary chamber.

Motivation

An ignition in an Ex”d” equipment can occur anywhere in the enclosure and the worst case scenario has to be identified. Previous experiments have been conducted to find the most favorable ignition position for propane in the PRSA by (Grovs 2010). Ethylene is more reactive gas than propane and most likely the two gases have different optimal ignition positions.

In the standardized test apparatus developed by The International Electrotechnical Commission (IEC) the MESG for ethylene is 0.65 mm. The MESG value may vary with different apparatus, and it is necessary to find the MESG for ethylene in the PRSA to investigate what effect other surface configurations have on the gap efficiency.

3.3.4 Optimal ignition position for re-ignition in the secondary chamber for slits with seven crosswise grooves

Experiments to find the optimal ignition position for re-ignition in the secondary chamber for slits with seven crosswise grooves have been carried out. The slit with surface configuration PH-7.2.3 was used throughout all experiments. Table 3-2 gives the specifications of the slit. The safe gap was found at each ignition position and the ignition position which gave the smallest safe gap was determined to be the most dangerous for a re-ignition in the secondary chamber.

Motivation

(Solheim 2010) showed that the most favorable ignition position for slits with crosswise grooves was the same as for undamaged slits with propane as the test gas. Ethylene gas explosion transmission might be more sensitive to changes in the surface configuration because of the high reactivity of ethylene. It is therefore necessary to investigate if adding crosswise grooves has an effect on the optimal ignition position for further experiments with different depth on the grooves in this work.

3.3.5 Flame gap surfaces with different depths on the multiple crosswise grooves

Experiments with crosswise grooves with different depth were carried out. Table 3-2 shows the specifications for the four slit sets.

Motivation

Previous experiments performed by (Grosv 2010) and (Solheim 2010) have shown that adding crosswise grooves to an undamaged surface increase the efficiency of the gap. The grooves were thought to create more turbulence in the jet of hot combustion products flowing out of the gap. The gas used in those experiments was propane. Ethylene is a more reactive gas with faster chemical kinetics, so it is necessary to investigate what effect increased turbulence by adding grooves will have on the probability for a re-ignition in the secondary chamber with this gas.

3.4 The Servomex 4200 Industrial Gases Analyser

A Servomex 4200 Industrial Gases Analyser was used to mix ethylene and air to the desired concentration. The gas analyzer measure the amount of oxygen and propane in a mixture, so when using ethylene as the fuel, the oxygen content was monitored. The oxygen concentration is measured with a paramagnetic oxygen sensor, which is a highly accurate technique for measuring vol. % oxygen. The oxygen molecules will be drawn to the strongest part of a magnetic field where two nitrogen-filled glass bulbs are placed on a rotatable dumbbell, due to the oxygen's paramagnetism. Nitrogen has opposite polarity and will be displaced by the oxygen so that the dumbbell will start rotating. An opposing current is applied to keep the dumbbell at its original position, and this current is directly proportional to the partial pressure of oxygen and is represented electronically as vol. % oxygen. (Henden 2011)

The calculations of the oxygen concentrations for the different ethylene/air mixtures investigated in this work are shown in Appendix B.

3.5 Measurement system and spark triggering

This chapter is based on chapter 3.8 in (Solheim 2010).

When the desired ethylene-air mixture was contained within the explosion apparatus a spark was generated in the primary chamber. The pressure in the primary chamber and the temperature in the secondary chamber were logged on a computer. Figure 3-12 shows the measurements system connected to the apparatus along with the spark generator and the "remote" which is used to trigger the spark.

3.5.1 Pressure measurements

In order to measure the explosion pressure in the primary chamber as a function of time $p_i(t)$, a piezoelectric transducer with a charge amplifier is mounted in the cylinder wall. The signal from the transducer is amplified by a Kistler 5015 Charge Amplifier. This signal is then logged in the LabView program on the computer. The pressure measurements were activated manually on the computer prior to each experiment.

3.5.2 Temperature measurements

It was performed temperature measurements for the experiments carried out with slits with multiple crosswise grooves. In order to measure the temperature of the hot combustion gases penetrating from the gap opening two thermocouples classified as type k is used. Type k thermocouples consist of a junction of two different metals. The junction creates a small voltage which increases with temperature. The signal was amplified through an operational amplifier (AD597) and logged on the computer.

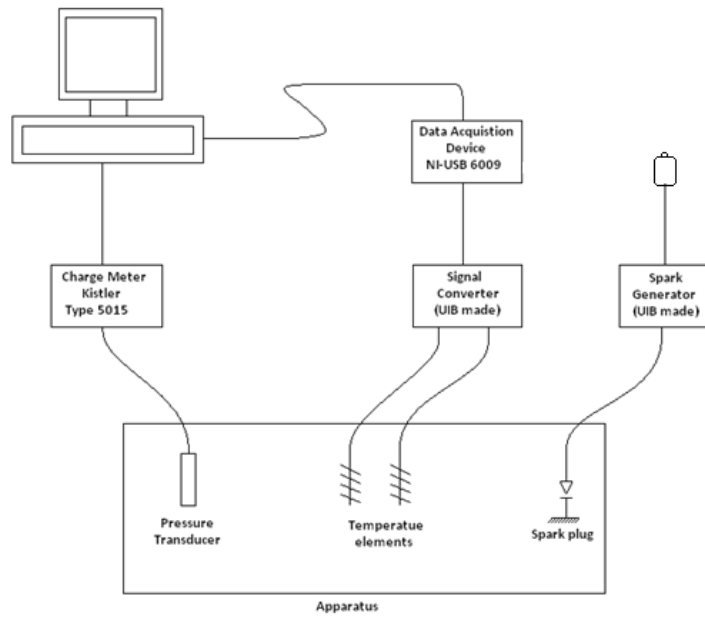


Figure 3-12 Measurement system and spark generator. Based on (Solheim 2010)

3.6 Sources of Error

This chapter is based on chapter 3.9 in (Solheim 2010),

3.6.1 Data Acquisition system

The experience from the work performed in this thesis shows that amplification of measured signal is important. One A/D converter reads all the channels and have switches inside the card which chooses which channel to read. If one channel is not satisfactorily amplified, then the signal from one channel would influence the signal from the next reading.

3.6.2 Gas concentration measurements

The uncertainty of the oxygen analyzer is 0.1% of the measured range of 0-100 vol. %, yielding an inaccuracy for measured concentrations of ± 0.1 . (Henden 2011)

The gas analyzer was calibrated for high values of oxygen with the air supply. This may lead to uncertainties in the measured oxygen concentration.

Another parameter which can have an influence on the actual gas concentration both in the primary and secondary chamber is that the mixture in the chambers may not always be homogenous.

3.6.3 Air humidity

The ethylene used in the experiments is mixed with pressurized air supplied from local distribution network. No measurements of humidity are done, but the air is filtrated and dried in a unit downstream the air compressor. In any case the quality of the air is not documented and pollution in form of oil, dust particles or water may exist in the supplied air. This may have effects on the results.

3.6.4 Pressure

There is uncertainty in the pressure readings due to the resolution of the pressure transducer. Kistler, the manufacturer of the piezoelectric transducer, states that the accuracy of the transducer is $\leq \pm 0.08\%$ of Full Scale Output when the calibration range is in the area of 0 to 25 bar. This gives an accuracy of ± 0.02 bar at the used measuring range, which is well within acceptable limits.

The pressure transducer is mounted a fixed distance at the vertical chamber wall of the primary chamber. The transducer may not detect local pressure gradients in the chamber.

3.6.5 Temperature

The thermocouples used in this work are not constructed to measure temperatures in explosions (or jets). The extremely rapid increase in temperature due to the explosion causes some uncertainty to the measured temperature, but it is assumed that the temperature difference measured between different experiments is valid.

3.6.6 Condensed water

After a few explosions water will typically condense on the inside of the walls of the primary chamber and may represent a significant source of error. Water may evaporate from the warm vessel walls during gas filling and the subsequent period of turbulence settling, altering the gas composition. Water in the gas mixture may affect reaction mechanisms and heat capacity, whereas a small portion of the water at the vessel walls may evaporate during the explosion. It is generally assumed that the explosions will be too rapid for significant amounts of water to evaporate.

3.6.7 Experiments

There are uncertainties due to construction tolerances in size of volumes, ignition positions and flange distances. In addition there is inaccuracy related to the experimental work, although good experimental procedures would counteract this, with reference to Appendix A.

The dimension of the distance "shims" is observed to have a variation of approximately ± 1 hundredths of a millimeter.

4 Experimental Results and Discussions

4.1 Experiments on rusted flame gap surfaces

Six sets of attached slits with a given gap opening were explosion tested with ten subsequent experiments before and after rusting.

The ignition position was 14 mm from the safe gap and the ethylene concentration in air was 6.52 vol. %. Some of the preliminary experiments are presented in Appendix D. The slits had gap openings from 0.68 mm to 0.75 mm.

Experiments with rusted slits were recorded with a high speed camera.

4.1.1 Results

Table 4-1 Comparison of the results from experiments performed before and after rusting.

Gap opening, Xi [mm]	Ignition position, Yi [mm]	Number of re-ignitions		Mean Pmax [barg]		Pmax first explosion test [barg]
		Undamaged	Rusted	Undamaged	Rusted	Rusted
0.68	14	0	0	1.63	3.48	3.77
0.69	14	0	0	1.60	3.49	3.82
0.70	14	2	0	1.54	3.44	3.77
0.71	14	6	3	1.48	3.42	3.83
0.72	14	8	0	1.57	3.61	4.07
0.75	14	10	6	1.48	3.21	3.93

From Table 4-1 it can be seen that the number of re-ignitions after the slits have been rusted has decreased. The slits with gap openings 0.68 mm and 0.69 mm gave re-ignitions neither before nor after rusting. The first re-ignitions with the rusted slits with gap openings 0.71 mm and 0.75 mm occurred after four and three explosion tests respectively. None of the rusted slits gave re-ignitions on the first out of ten explosion tests.

The slit with gap opening of 0.70 mm gave two re-ignitions at undamaged state. This is conflicting with the results from experiments conducted to find the most favorable ignition position for an undamaged slit in section 4.3. The distance shims were cut to fit the height of the slits and may have been folded in the edges, which could have resulted in a wider gap opening.

Pressure measurements before rusting showed abnormally low values compared with results from experiments conducted on undamaged slits later in this work. This may be due to incorrect settings in the Labview program. Table 4-2 shows a comparison of pressure measurements after rusting and for experiments carried out on undamaged slits with an ignition position of 14 mm later in this work.

Table 4-2 Comparison of pressure measurements for undamaged slits later in this work and rusted slits.

Gap opening, Xi [mm]	Mean Pmax [barg]	
	Undamaged slits at later experiments	Rusted
0.68	3.54	3.48
0.69	3.67	3.49
0.70	3.52	3.44
0.71	3.34	3.42
0.72	3.54	3.61
0.75	N/A	3.21

The differences in the mean maximum pressures for undamaged slits later in this work and on the rusted slits are not significant. On this basis it is assumed that the mean maximum pressure before and after corrosion is similar.

From Table 4-1 it is shown that the maximum explosion pressure on the first explosion is significantly higher than the mean maximum pressure for ten subsequent experiments on each rusted slit. This is in accordance with the pressure measurements (Solheim 2010) obtained from experiments on rusted slits with propane as the test gas. Figure 4-1 shows the maximum pressures of ten subsequent experiments performed on the rusted slit with gap opening of 0.72 mm. The pressure decreases rapidly from the first explosion test to the third before it tends to stabilize at approximately 3.5 barg for the last five experiments. The same kind of reduction in pressures was also observed for the other slits.

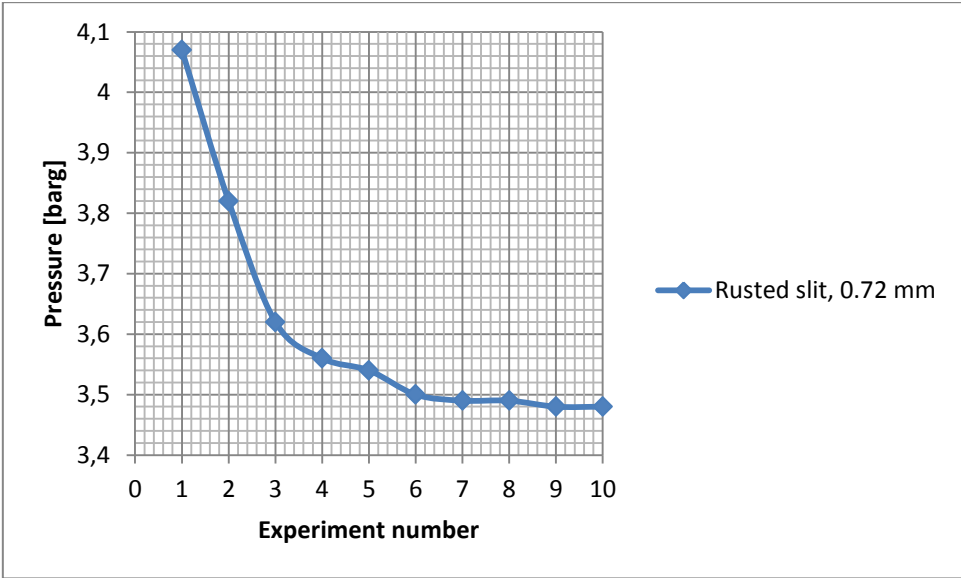


Figure 4-1: Pressure due to ten subsequent explosions with rusted gaps surface. Gap opening 0.72 mm.

After corrosion the gap opening was blocked by rust, and a great amount of rust was blown out of the gap opening during the first explosion test. Figure 4-2 shows the gap opening of a rusted slit before and after ten subsequent explosion tests. It can be seen that the gap opening has increased after ten experiments.



Figure 4-2 Rusted slit at gap opening 0.72 mm before (to the left) and after (to the right) ten subsequent explosion tests.

From the high speed camera recordings it was observed, which are assumed to be, glowing rust particles blown out of the slit on the first explosions tests on the rusted slits, see Figure 4-3 and Figure 4-4. During the first explosion test on the rusted slits it was not observed re-ignition.



Figure 4-3 High speed camera recording of first explosion test on rusted slit with gap opening 0.71 mm. No re-ignition.



Figure 4-4 High speed camera recording of second explosion test on rusted slit with gap opening 0.71 mm. No re-ignition.

Figure 4-5 shows a sequence of frames which were recorded of a re-ignition on the rusted slit with gap opening 0.71 mm. From this observation it seems to be the hot combustion products penetrating through the slit which ignites the gas in the secondary chamber, and not the glowing rust particles.



1



2



3



4

Figure 4-5 High speed camera recording. Re-ignition with rusted slit of gap opening 0.71 mm. 300 frames/second.

4.1.2 Discussion

The slits were placed midway between low and high tide, which according to Figure 2-30 is the zone with the highest corrosion rate. Figure 2-29 shows that the corrosion process “eats” up the surface and creates elevations of rust. Since the slits were attached with relatively small gap openings, the rust was not washed away during the time they corroded as it would have done if the slits had been corroded separately. The rust which was building up on the surface got compressed between the two slits due to the compressibility of rust. After ten explosion tests only the outer layer of rust had been blown out and it seems that the bond strength between steel surface and rust are strong. The slits which gave zero re-ignitions at undamaged state, did not give any re-ignitions after rusting. This means that the gap openings were not wider than at undamaged state even after a great amount of rust had been blown out.

As can be seen from Figure 4-1 the maximum pressure decreased during ten consecutive explosions. This is consistent with the observation of rust being blown out of the slits. The venting area increased and therefore the pressure decreased. The slits which gave re-ignitions at undamaged state gave less re-ignition after rusting. The re-ignitions occurred after three and four previous explosion test, see Appendix D. A sufficient amount of rust had then been blown out, which caused a re-ignition by the hot combustion products possible.

In the work performed by (Solheim 2010) on slits which had corroded for three months, a significantly higher mean maximum pressure after rusting was observed. Solheim argued that this could be due to an increased roughness, which increased the resistance through the slit. In this work, the slits were corroded for a shorter period of time leading to less roughness on the surface. This may explain why the mean maximum pressure comparisons of the undamaged slits did not show significant differences from the rusted slits.

In the work performed by (Solheim 2010) he did not observe any re-ignitions on the rusted slits. A shorter corrosion time gives less compact rust in the gap opening, which is probably the reason why it was observed re-ignitions in this work on two of the rusted slits. This indicates that a longer corrosion time increases the efficiency of the gap.

In Figure 4-3 and Figure 4-4 it is assumed to be glowing rust particles which flow out of the gap opening. The color is red/orange. This indicates a low temperature, which might explain why the gas was not ignited in the secondary chamber. From Figure 4-5, which shows a re-ignition in the secondary chamber, it seems to be the jet of hot combustion products from the primary chamber that ignites the gas. One can see that the color is more blue than red/orange and this means a higher temperature.

The probability of ten subsequent explosions in a flameproof enclosure occurring in real life is low. It is therefore the first explosion test which is most important. No re-ignition was observed on the first experiment, even for the slit which gave 100 % re-ignition at undamaged state. This means that rust increased the efficiency of the gap.

4.2 Experiments to find the most dangerous concentration of ethylene for re-ignition in the secondary chamber

A total of 60 experiments were carried out to find the concentration which gives most re-ignitions in the secondary chamber. To limit the number of experiments, six concentrations of ethylene were chosen under and above the stoichiometric value of 6.52 vol. % ethylene in air. The ignition position was chosen to be 25 mm from the gap opening.

The concentrations of ethylene which were investigated were 6.2 vol. %, 6.5 vol. %, 6.6 vol. %, 6.7 vol. %, 6.8 vol. % and 7.0 vol. %. The maximum pressure was measured in all of the experiments.

4.2.1 Results

The concentration that gave most re-ignitions in ten subsequent experiments was determined. The results from the experiments are plotted in Figure 4-6.

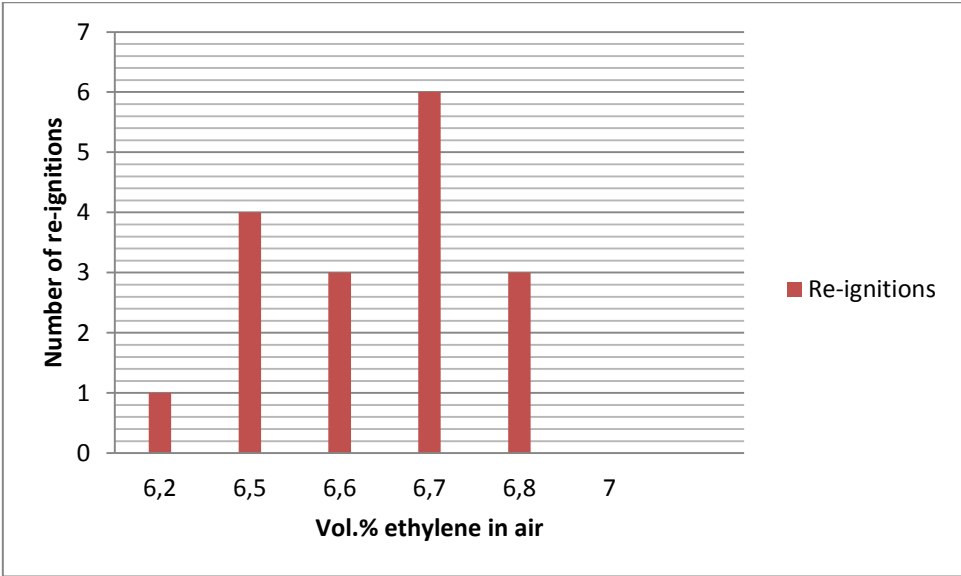


Figure 4-6 Concentration of ethylene in air giving most re-ignitions in the secondary chamber. All experiments were conducted with a gap opening of 0.69 mm and an ignition distance from the gap opening of 25 mm.

Figure 4-6 shows that the concentration of 6.7 vol. % ethylene in air gave most re-ignitions in the secondary chamber, with a total of six re-ignitions. This concentration was therefore determined to be the most dangerous one, and was used throughout the rest of the experimental work in this investigation.

Table 4-3 shows that the variations in the mean maximum pressures are not significant.

Table 4-3 Mean maximum pressure in experiments performed with different concentrations of ethylene. Ten subsequent experiments were conducted with each concentration.

Date	22.03.2012-26.03.2012
Surface configuration	Undamaged
Ignition position, Xi [mm]	25
Gap with, Yi [mm]	0,69
Vol. % ethylene in air	Mean maximum pressure [barg]
6.2	3.51
6.5	3.62
6.6	3.55
6.7	3.63
6.8	3.58
7.0	3.62

4.2.2 Discussion

Figure 2-9 obtained from (Beyer 1996), where the safe gap is a function of the concentration, the safe gap is smallest at approximately 6.8 vol. % ethylene in air. For leaner and richer mixtures the safe gap increases. The results from this work are therefore in good agreement with previous experimental work, where a slightly richer concentration is found to be the most dangerous.

There was not observed any significant change in the pressure measurements. The reason for the small variations is probably due to the relatively small range of concentrations which were tested. In the work performed by (Larsen 1998), where he tested concentrations in the range of approximately (4.2 ± 2) vol. % propane in air, there was a clear decrease in the pressure for leaner and richer mixtures, see Figure 2-23.

From Figure 2-4 it is seen that the laminar burning velocity is highest at approximately 7 vol. % ethylene in air, which is close to the most dangerous concentration found in this work. The laminar burning velocity is an indication of the reactivity of a gas. A slightly richer concentration in the secondary chamber will therefore favor a re-ignition in the secondary chamber.

4.3 Experiments to find the optimal ignition position for re-ignition in the secondary chamber with undamaged slits, and the MESG for ethylene

Several experiments were performed to find the safe gap at each ignition position. The smallest safe gap was determined to be the MESG, and the corresponding ignition position to be the most favorable for a re-ignition in the secondary chamber.

The ignition positions examined were: 5 mm, 10 mm, 14 mm, 20 mm, 25 mm, 30 mm and 35 mm from the gap opening. A concentration of 6.7 vol. % ethylene was used through the entire experiment.

4.3.1 Results

The largest gap opening which gave no re-ignitions in the secondary chamber in ten subsequent experiments was determined for each ignition position. The results are presented in Figure 4-7.

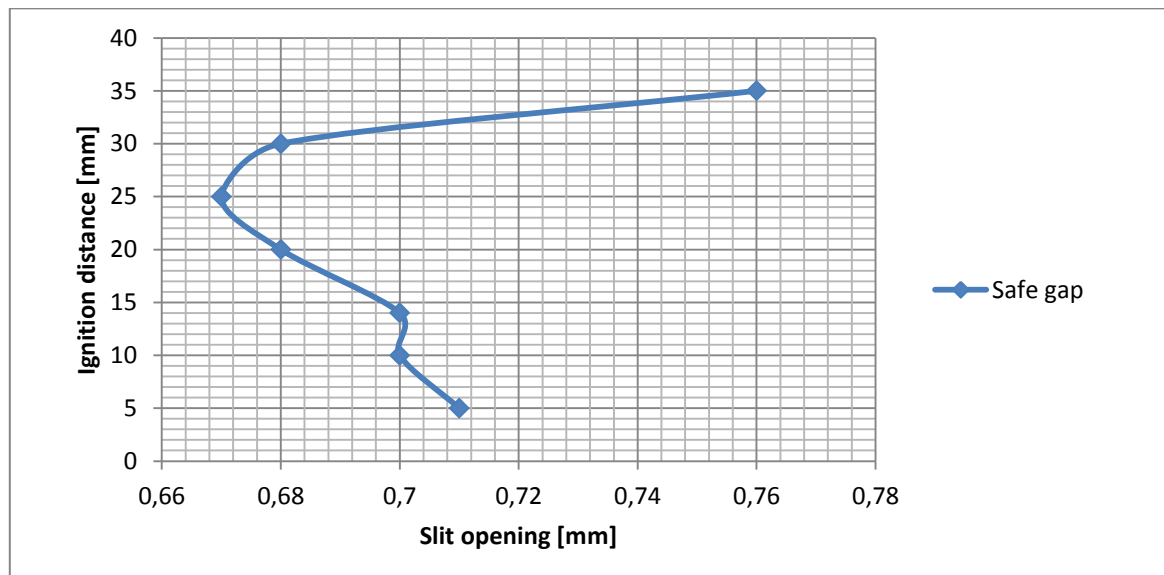


Figure 4-7 Optimal ignition position for re-ignition in the secondary chamber for an undamaged gap surface. The blue dotted line represents the largest gap opening that gave no re-ignition in the secondary chamber in ten subsequent experiments. All experiments were performed with 6.70 vol. % ethylene in air.

From Figure 4-7 it can be seen that the ignition position of 25 mm from the gap opening gave the smallest safe gap and is therefore determined to be the optimal ignition position. Thus the safe gap of 0.67 mm was determined to be the MESG for ethylene in the PRSA. Plotting the results gave a C-curve which is in accordance with previous work in relation to the most optimal ignition position, see section 2.4. Figure 4-8 shows the comparison with the C-curves obtained with propane in the work performed by (Grosv 2010).

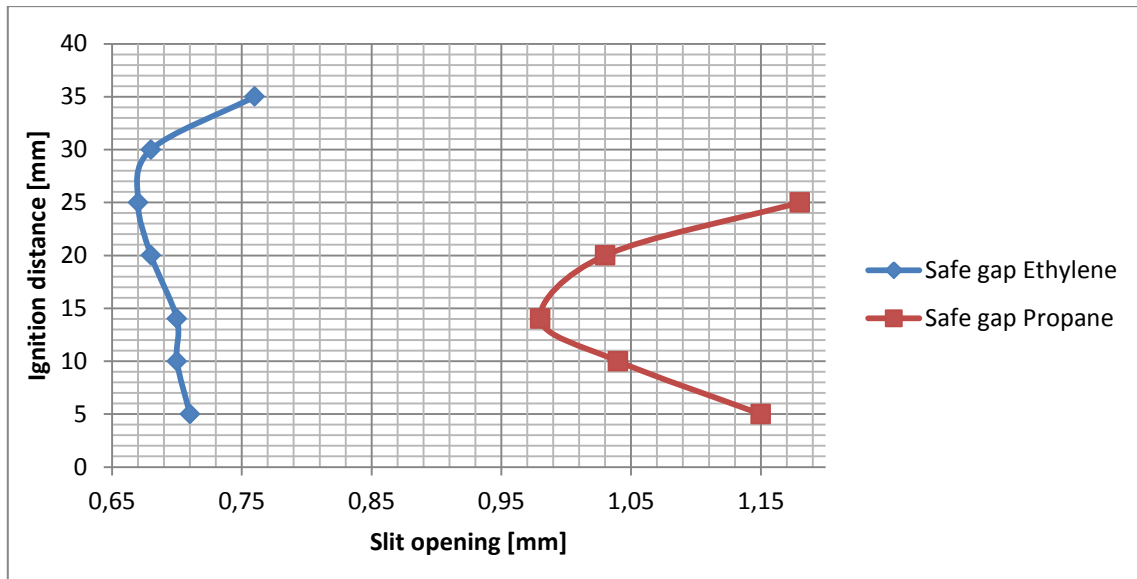


Figure 4-8 Comparison of the safe gaps at each ignition position for ethylene and propane with undamaged slits. The values for propane are from (Grosv 2010).

The C-curve for propane is placed far to the right. This was expected because ethylene is a more reactive gas than propane and has a smaller MESG value, see Table 2-6. It is seen that the optimal ignition position is not equal for the two gases. The ignition position had to be moved further away from the gap opening to obtain the most favorable conditions for re-ignition in the secondary chamber for ethylene gas explosions.

Ten subsequent experiments with a constant gap opening of 0.69 mm were carried out on each ignition position to compare the mean maximum pressures in the primary chamber. The results are shown in Table 4-4.

Table 4-4 Mean maximum pressure and number of re-ignitions for experiments with different ignition position and gap width 0.69 mm. Ten experiments were conducted for each ignition position.

Date	26.03-2012-04.05.2012	
Surface configuration	Undamaged	
Gap width, X_i [mm]	0.69	
Ignition position, Y_i [mm]	Mean Pmax [barg]	Number of re-ignitions
5	3.31	0
10	3.31	0
14	3.37	0
20	3.53	4
25	3.63	6
30	3.34	4
35	3.41	0

Table 4-4 shows that the mean maximum pressure increased when moving the ignition position from 5 mm to 25 mm from the gap opening.

The pressure decreased for ignition position 30 mm and 35 mm. The ignition position of 25 mm gave most re-ignitions in the secondary chamber, which verifies that this is the optimal ignition position for re-ignition in the secondary chamber.

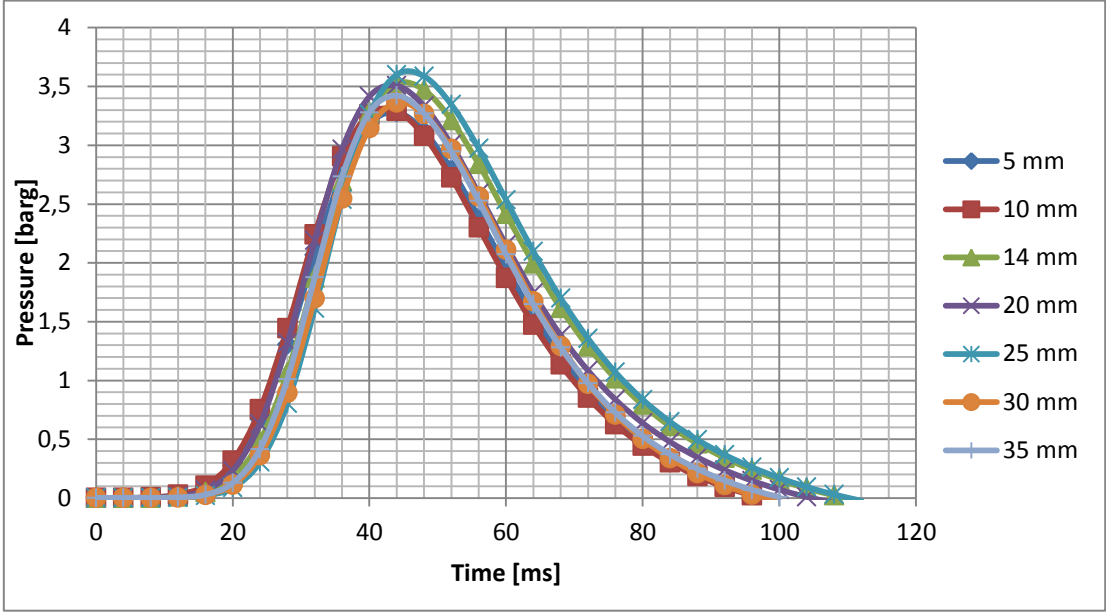


Figure 4-9 Pressure versus time in the primary chamber for different ignition positions when venting through an undamaged slit at constant gap opening of 0.69 mm.

Figure 4-9 shows the pressure versus time at different ignition positions with a constant gap opening of 0.69 mm. The pressure build-up is approximately the same at each ignition position.

4.3.2 Discussion

Factors like the pressure build-up in the primary chamber, heat loss, velocity of the jet and turbulence build-up above the gap opening in the secondary chamber influence the probability of a re-ignition in the secondary chamber. Moving the ignition position has an effect on these factors.

The pressure decreased when moving the ignition source from 5 mm to 25 mm from the gap opening. Previous experimental work performed by (Larsen 1998) has also shown that the maximum pressure increased with increasing ignition distance from the safe gap. From the Schlieren pictures shown in Figure 2-6 it can be seen that when the gas in the 1 liter primary chamber, which is the same chamber as in the PRSA used in this work, is ignited close to gap opening the flame front reaches the walls of the chamber at an earlier stage than when it is ignited closer to the center. When a flame front reaches the wall there will be chain terminating reactions, see section 2.1.1. Radicals will diffuse into the wall which leads to a slower combustion process of the rest of the unburned gas. At an ignition position close to the center the flame front develops as a spherical fire ball throughout the entire volume and the diffusion of radicals into the walls of the chamber will occur at later stage. This results in a faster combustion. The faster the combustion rate, the higher the maximal explosion pressure in the primary chamber. When the ignition position is close to the gap opening less cold gas, ahead of the flame front, has to be pushed through the slit. Cold gas has a higher density than

hot gas and requires a greater force to be pushed through the slit. These factors may explain why the pressure increases when the ignition source is moved away from the gap opening and provides a reason for assuming that the pressure measurements for ignition position 30 mm and 35 mm are abnormal and should be disregarded.

Redeker (Redeker 1981) suggested a transition from laminar to turbulent flow in the hot combustion products which flows out of the gap opening as the ignition source is moved towards the center of an internal chamber. The results in this work correlate to some extent this assumption. When the ignition source is close to the gap entrance, less combustion products flow through the slit per millisecond because of the interrupted combustion by walls, which gives more time for cooling in the primary chamber and the slit. As the ignition position is moved further into the primary chamber the flux of combustion products through the slit increases and a greater amount of hot gas can react with the unburned gas in the secondary chamber. Consequently the safe gap decreases. A further increase in the ignition distance will cause the jet to have greater velocity due to a higher pressure. A high velocity of the jet will increase the turbulence level above the gap opening and the heat loss will exceed the heat generation due to a better mixing between hot and cold gas. Thus the safe gap increases. An ignition position of 25 mm from the safe gap is a critical ignition point where the relationship between pressure, velocity and turbulence level creates optimal conditions for re-ignition in the secondary chamber.

Ethylene is a more reactive gas than propane. This leads to smaller safe gaps for ethylene as shown in Figure 4-8. The optimal ignition distance for re-ignition in the secondary chamber is longer for ethylene than propane. This is in accordance with the work by (Redeker 1981) where the safe gap was investigated as a function of the ignition distance for different gases. From Figure 2-9 it is shown that the smallest safe gap for ethylene is obtained at longer distance from the gap opening than methane. Methane is, as propane, classified as a group IIA gas and hence less reactive than ethylene, see Table 2-5. The fact that ethylene has faster chemical kinetics makes it more "tolerable" for turbulence and may explain why the most favorable ignition position for ethylene is further away from the gap opening than for propane.

4.4 Experiments to find the optimal ignition position for re-ignition in the secondary chamber for slits with seven crosswise grooves

Experiments were carried out with the gap surface of configuration PH-7.3.2 (see section 3.2.1) to determine which ignition point gave the smallest safe gap. This point is characterized as the optimal ignition position for a re-ignition in the secondary chamber.

The ignition positions examined were 2 mm, 5 mm, 10 mm, 14 mm, 20 mm and 25 mm from the gap opening.

To compare the pressure development for the different ignition positions, experiments with a constant gap opening of 0.74 mm were carried out. Ten subsequent experiments were executed on each ignition position.

4.4.1 Results

The largest gap opening that gave no re-ignitions in the secondary chamber in ten subsequent experiments was determined at each ignition position. The results are plotted in Figure 4-10.

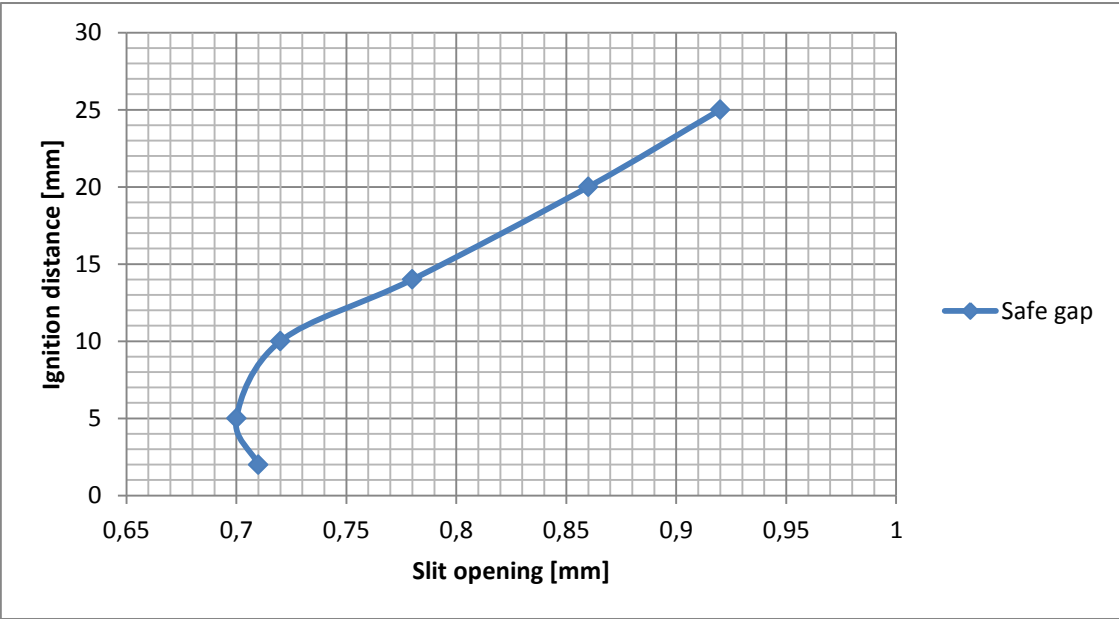


Figure 4-10 The optimal ignition point for re-ignition in the secondary chamber in experiments with multiple crosswise grooves (PH-7.2.3). The blue dotted line represents the largest gap opening that gave no re-ignition in the secondary chamber in ten subsequent experiments. All experiments were performed with 6.70 vol. % ethylene in air.

Figure 4-10 shows that the safe gap decreases with decreasing ignition distance from the safe gap, down to the point 5 mm from the gap opening. When the ignition position is moved to 2 mm from the gap opening, the safe gap increases slightly. The most favorable ignition position is therefore determined to be 5 mm, and is used throughout all experiments for slits with seven crosswise grooves.

Figure 4-11 shows the comparison of the safe gaps obtained for the undamaged slit and the slit with seven crosswise grooves. The two surface configurations have different optimal ignition position. It is seen that for ignition distances 25 mm, 20 mm and 14 mm the safe gap is significantly wider for the slit with crosswise grooves than for the undamaged slit. For shorter distances, 10 mm and 5 mm, the difference is not significant.

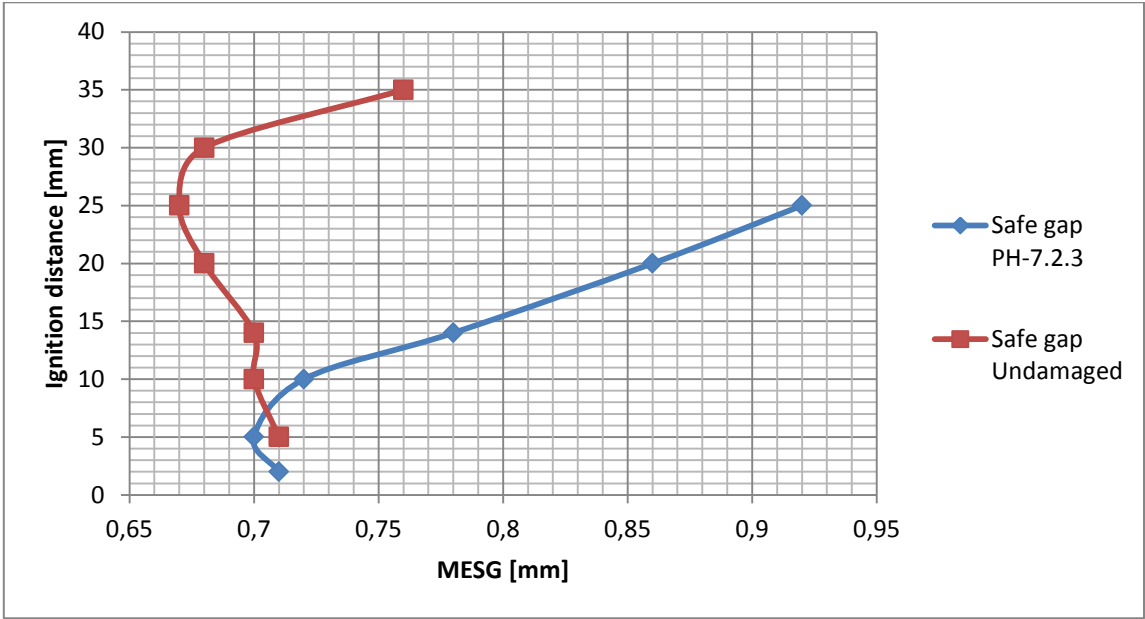


Figure 4-11 Comparison of the safe gaps at some ignition points for an undamaged slit and the slit with surface configuration PH-7.2.3 Mixture of 6.7 vol. % ethylene in air.

An interesting observation from Figure 4-11 is that the safe gap is smaller for the slit with crosswise grooves than for the undamaged slit, at ignition distance 5 mm from the flame gap. This is discussed in Section 4.5.2 on experiments performed with different depths on the crosswise grooves compared to the undamaged slit.

Figure 4-12 compares the safe gaps at different ignition positions obtained for ethylene in this work and for propane in previous works, (Grosv 2010; Solheim 2010), with the undamaged slit and the slit with seven crosswise grooves. The curves from experiments performed with propane are placed to the right in relation to the curves for ethylene. This was expected because ethylene is a more reactive gas than propane and has a lower MESG value.

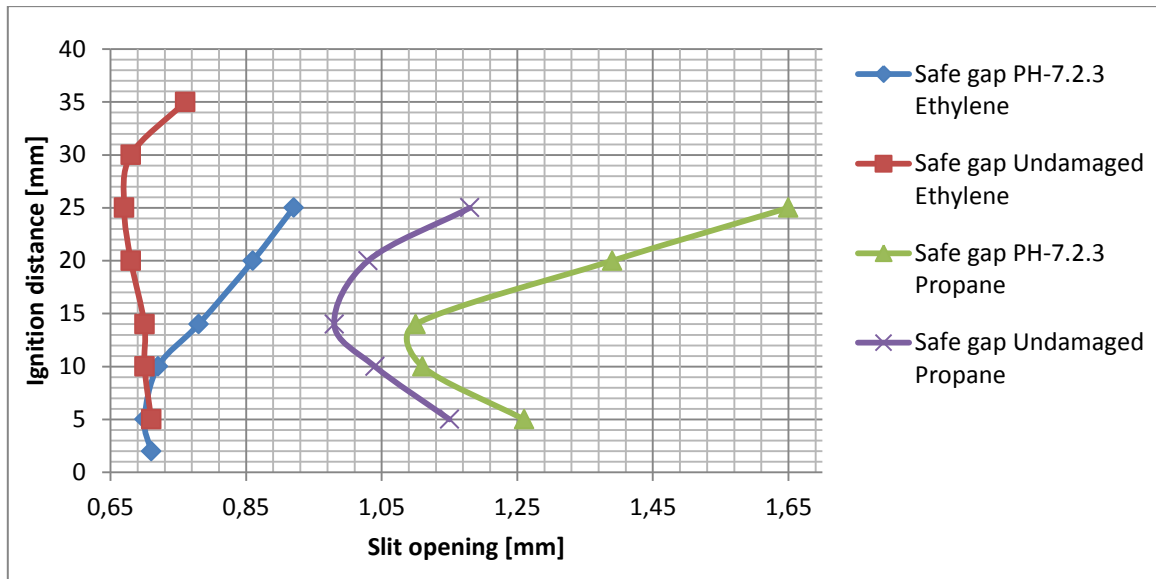


Figure 4-12 Comparison of the largest gap openings giving no re-ignition at some ignition distances for an undamaged slit and slit with surface configuration PH-7.2.3 for ethylene and propane. The values for propane are obtained from (Grosv 2010; Solheim 2010).

It is seen that the most favorable ignition position for the undamaged slit and the slit with crosswise grooves are equal when using propane as test gas. Solheim suggested that this would indicate similar physical phenomenon is applicable for the two surface configurations. This assumption cannot be drawn from results with ethylene because the ignition positions for the two slits are different. Adding crosswise grooves seems to have a much greater effect on the optimal ignition position for a re-ignition in the secondary chamber for an ethylene gas explosion than propane explosion.

Table 4-5 shows the mean maximum pressure in the primary chamber and number of re-ignitions at each ignition position, with a constant gap opening for the slit with seven crosswise grooves.

Table 4-5 Mean maximum pressure and number of re-ignitions for experiments with surface configuration PH-7.2.3 at different ignition positions. Ten experiments were conducted on each ignition position.

Date	12.04.2012-12.05.2012	
Surface configuration	PH-7.2.3	
Gap width, X_i [mm]	0,74	
Ignition position, Y_i [mm]	P_{max} mean [barg]	Number of re-ignitions
2	3,62	10
5	3,70	10
10	3,69	4
14	3,66	0
20	3,68	0
25	3,70	0

There is no clear pattern in the mean maximum pressures from the ignition position of 2 mm to 25 mm from the safe gap. This differs from earlier observations in this and previous work

where the pressure has increased with increasing ignition distance. It is also seen by the number of re-ignitions observed when the gap opening was constant that an ignition position close to the gap opening favors a re-ignition in the secondary chamber.

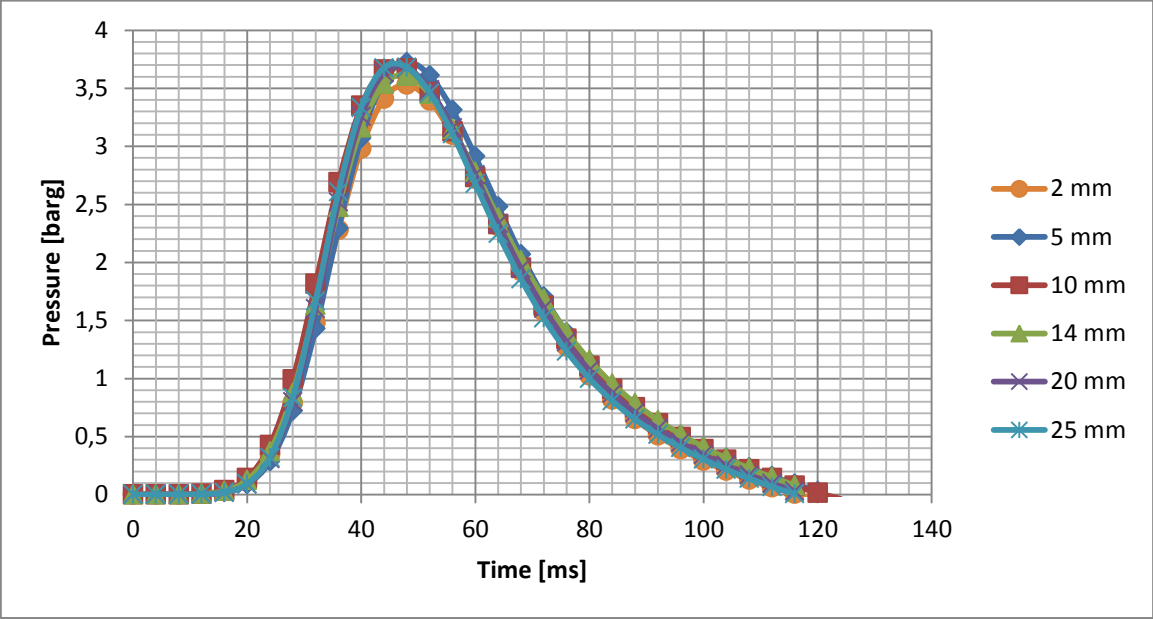


Figure 4-13 Pressure versus time in the primary chamber at different ignition positions when venting through slits with crosswise grooves with a constant gap opening of 0.74 mm.

Figure 4-13 shows that there is no distinct difference in the pressure developments for when igniting at different ignition positions in the primary chamber for slit with crosswise grooves.

4.4.2 Discussion

The pressure measurements at the different ignition positions with constant gap openings showed no major variations and it is difficult to explain the reason for this. Adding grooves to the slit will result in a change of the flow of the hot combustion products through the slit, but it is assumed that the combustion process in the primary chamber is the same as for experiments with undamaged flame gaps, and that changing the ignition position has the same effect on the combustion process as discussed in section 4.3.2.

The comparison in Figure 4-11 between the safe gaps at different ignition positions for an undamaged slit and a slit with crosswise grooves indicates that more turbulence is generated with grooves. When the gas is ignited at long distances from the safe gap the grooves may create fluctuations in the unburned gas which is pushed through the slit ahead of the flame front. This will cause a turbulent state in the arrival of the jet of the hot combustion products in the secondary chamber. The grooves will also create more fluctuations in jet which is thought to have a high velocity due to fast combustion rate when igniting the gas at relatively long distances from the gap, as discussed in section 4.3.2. Consequently a high level of turbulence is generated in the secondary chamber which causes an efficient cooling of the hot combustion products by the cold gas. When the ignition source is moved closer to the gap opening, less unburned gas is pushed through the slit and the flame front in the primary chamber reaches the gap opening at an earlier stage. A lower level of turbulence has then been generated when the jet arrives the secondary chamber. The flux of hot combustion products

through the slit is thought to decrease when moving the ignition position closer to gap opening and the jet will have a lower velocity which also contributes to a decrease in the turbulence level. Hence the safe gap must be smaller. This may explain why an ignition position close to the safe gap, which gives less turbulence in the secondary chamber, is the most favorable ignition position for slits with crosswise grooves.

The small differences in the safe gaps for the two slits when the ignition source is close to gap opening is discussed in section 4.5.2.

When the ignition position is moved to 2 mm from the gap opening the safe gap increased slightly. Ignition so close to gap opening will, as discussed in section 4.3.2, leads to a slower combustion of the entire volume in the primary chamber. The hot combustion products may therefore have more time to be cooled in the primary chamber. In addition, adding grooves increases the surface area inside the slit, and when the grooves creates fluctuations in the flow there will be an increase in the contact area between the hot gas and the cold walls. This may result in a lower temperature of the jet as it penetrates into the secondary chamber.

As can be seen from Figure 4-12 the most favorable ignition point for re-ignition in the secondary chamber is similar for undamaged slits and slits with crosswise grooves when propane is used as the test gas. Ethylene is a more reactive gas with smaller safe gaps which causes a larger maximum explosion pressure in the primary chamber. In general this will lead to a higher velocity of the jet into the secondary chamber. This might be the reason why adding crosswise grooves give different optimal ignition positions than at undamaged state for ethylene explosions and not for propane explosions.

4.5 Experiments with different depths on the multiple crosswise grooves

Several experiments were performed on each slit configuration to find the different MESG values. The largest gap which gave no re-ignitions in the secondary chamber in ten subsequent explosions is determined to be the MESG.

Experiments with a constant gap opening of 0.70 mm were conducted on each different slit, including the undamaged slit, for comparison of pressure and temperature measurements. The temperature was measured at five out of ten subsequent experiments on each slit.

The most dangerous ignition position for a re-ignition in the secondary chamber for slits with crosswise grooves found in section 4.4, was used in all of the experiments.

4.5.1 Results

Table 4-6 MESG values and mean maximum pressures for slits with different depths on the seven crosswise grooves.

Date	26.04.2012-28.04.2012		
Surface configuration	Ignition position, Yi [mm]	MESG [mm]	Mean Pmax at MESG [barg]
PH-7.2.3	5	0.70	3.70
PH-7.2.2	5	0.71	3.55
PH-7.2.1	5	0.70	3.47
PH-7.2.0,5	5	0.67	3.56
Undamaged	5	0.71 (safe gap)	3.29
Undamaged	25	0.67	3.11

Table 4-6 shows the MESG values for the slits with different depth on the crosswise grooves compared to the safe gap for an undamaged slit and the MESG value for an undamaged slit found in section 4.3. The results showed no clear correlation between the depths of the crosswise grooves and the MESG values. This is in accordance with the results (Solheim 2010) found in his experiments with propane as the test gas.

The safe gap for an undamaged slit at the ignition position of 5 mm is larger and equal to the MESG values for slits with seven crosswise grooves. The MESG values for slits with crosswise grooves are not smaller than the MESG found for ethylene in section 4.3 for an undamaged slit.

Table 4-7 shows the results from the pressure and temperature measurements for the different slits with an equal gap opening of 0.70 mm.

Table 4-7 Mean maximum pressures and mean temperature for slits with different depths on the crosswise grooves and an undamaged slit. All slits had a gap opening of 0.70 mm. The temperature was measured at an altitude of 2 cm above the gap opening in the secondary chamber.

Date	26.04.2012-28.04.2012				
Surface configuration	Ignition position, Yi [mm]	Gap width, Xi [mm]	Mean Pmax [barg]	Mean Temp. [°C]	Number of re-ignitions
PH-7.2.3	5	0.70	3.70	82	0
PH-7.2.2	5	0.70	3.55	80	0
PH-7.2.1	5	0.70	3.47	100	0
PH-7.2.0,5	5	0.70	3.51	294	10
Undamaged	5	0.70	3.36	170	0

The mean maximum pressure decreases with decreasing depth of 3 mm to 1 mm. A depth of 0.5 mm gave a slight increase in the pressure compared to the slit with a depth of 1 mm on the crosswise grooves. All the pressure measurements for the slits with crosswise grooves were larger than for an undamaged slit.

The temperature measurements do not show the correct temperature because the battery in the signal amplifier for the thermocouples had low voltage during the experiments. The real temperature is probably higher than what was measured. It is still assumed that the ratio between temperatures measured for the different surface configurations can be considered.

It can be seen from Table 4-7 that the slit with surface configuration PH-7.2.3 and PH-7.2.2 showed approximately 50% lower temperature compared to an undamaged slit. One surprising result was that the grooves of depth 0.5 mm showed the highest temperature. This is also the slit which had the same MESH value as for an undamaged slit, and it was the only slit which gave re-ignitions in the secondary chamber during experiments with a constant gap opening.

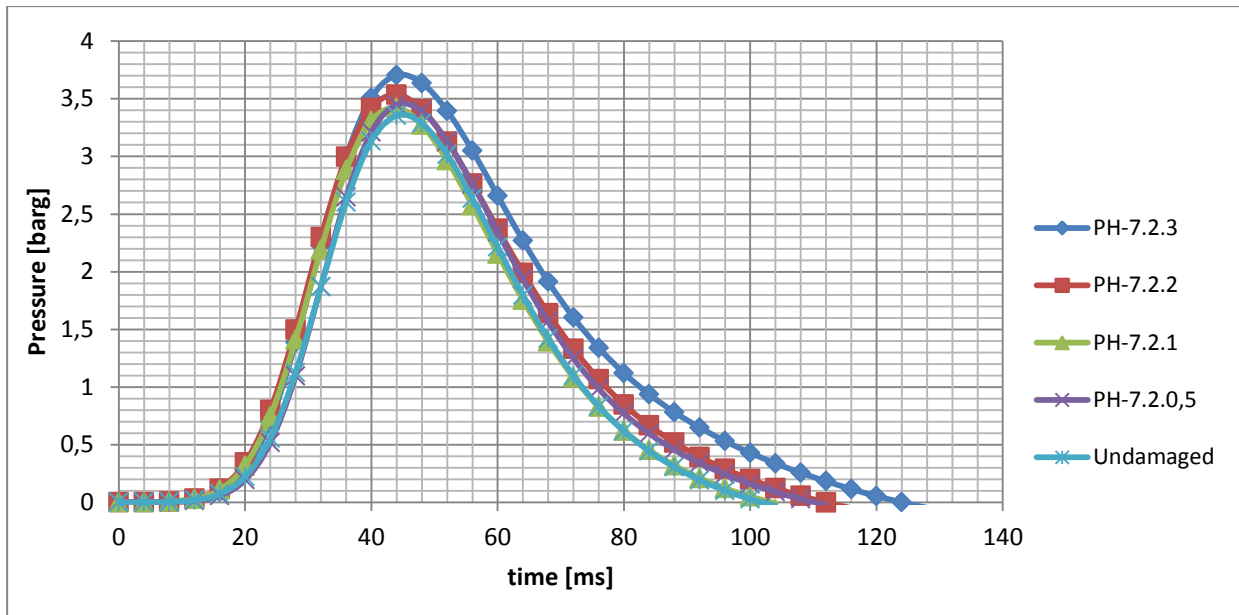


Figure 4-14 Pressure versus time for the slits with seven crosswise grooves compared to an undamaged slit. The gap opening and ignition position is constant at 0.70 mm and 5mm respectively.

The pressure development in Figure 4-14 for the different surface configurations showed that time spent to reach a gauge pressure of zero after the maximum pressure was obtained, is longest for the slit with deepest crosswise grooves, PH-7.2.3.

4.5.2 Discussion

Pressure measurements at constant gap opening showed that the slits with crosswise grooves gave a higher maximum explosion pressure in the primary chamber than for undamaged slits. This is in accordance with theory reviewed in section 2.3.4 where an increase in the surface roughness gave a higher friction factor. A higher friction factor leads to greater resistance through the slit and the flow of combustion products will decrease through the gap. From Figure 4-14 it can be seen that the time from the maximum pressure was achieved to the pressure reached a gauge pressure of zero in the primary chamber was longer for experiments performed with the deepest crosswise grooves than for an undamaged slit. This means that it takes longer for the combustion products to leave the primary chamber. This is also supported by the results obtained for experiments on crosswise grooves with propane as the test gas (Solheim 2010).

The temperatures above the slits in the secondary chamber were lower for all of the slits with crosswise grooves than for an undamaged slit, except the slit with 0.5 mm deep grooves. This indicates that the heat loss is greater when grooves are added, which may support the work performed by (Ceylan and Kelbaliyev 2003). The roughness will create turbulence and increase the contact area between the hot combustion products and the cold walls and the heat transfer will increase. The fluctuations will also cause a better mixing between hot and cold gas which may lead to a lower temperature. The slit with grooves of depth 0.5 mm was the only slit which gave re-ignitions in the secondary chamber when the gap opening was constant, which explains why the temperature measured was highest for this slit.

Since the grooves creates fluctuations in the flow it will lead to that more unburned gas in the secondary chamber is mixed with the hot gas coming out of the gap opening. More ethylene molecules will be in contact with hot combustion products. Ethylene is a highly reactive gas with fast chemical kinetics due to its double bonds. The more ethylene molecules which react, the more energy is released. Heat generation will occur faster than the cooling by the cold gas in the secondary chamber, unless the turbulence intensity is sufficiently high. The slit with grooves of 0.5 mm is thought to create less turbulence than the slits with crosswise grooves due to the low MESH value. The reason why the MESH value for this slit is smaller than the safe gap for an undamaged slit may be due to a better mixing and hence more ethylene can react because of the fluctuations caused by the grooves.

A better mixing due to turbulence together with the fast chemistry of ethylene compensates for the increased heat loss in the slit with crosswise grooves and may be the reason why the MESH values for the slits with deepest crosswise grooves are not significantly different from the safe gap for an undamaged slit.

The MESH value found for an undamaged slit in section 4.3 is 0.67 mm. None of the slits with crosswise grooves gave a MESH value smaller than this. This means that the efficiency of the gap by adding crosswise grooves is not reduced, which is consistent with previous work performed by (Grosveld 2010) and (Solheim 2010) on the same slits and with propane as the test gas.

It should be mentioned that all of the experiments were conducted at the most favorable ignition position for the slit with surface configuration PH-7.2.3. As can be seen from the results obtained in section 4.4 there are great differences in the most favorable ignition position for the undamaged slit and the slit with deepest crosswise grooves. The results from this section indicate that different depths on the grooves creates different degrees of turbulence, which might result in different optimal ignition positions for a re-ignition in the secondary chamber for the four slits.

5 Conclusion

1. Rusted slits

Six slits with rusted gap openings were explosion tested prior and after rusting. None of the rusted slits, which gave zero re-ignition at undamaged state, gave re-ignitions during ten explosions tests on each slit. The slits which gave re-ignitions at undamaged state gave less re-ignition after rusting. None of the rusted slits gave re-ignition on the first explosion test, which is the most important test. The main conclusion is that rust increased the efficiency of the safe gap.

2. Preliminary experiments

Preliminary experiments were conducted to find the “worst case” scenario for undamaged slits and slits with seven crosswise grooves.

- The most favorable concentration for re-ignition in the secondary chamber was found to be 6.7 vol. % ethylene in air. This is in accordance with reviewed literature where a slightly richer concentration gives the smallest safe gap.
- The optimal ignition position for a re-ignition in the secondary chamber with undamaged flame gaps was found to be 25 mm from the gap opening. At this point the safe gap was 0.67 mm and was determined to be the maximum experimental safe gap (MESG) for ethylene in the Plane Rectangular Slit Apparatus.
- The optimal ignition position for a re-ignition in the secondary chamber for slits with seven crosswise grooves was found to be 5 mm from the gap opening. The results indicated that the grooves caused a great deal of turbulence and that a lower degree of turbulence is obtained when the ignition position is close to the gap entrance.

3. Slits with multiple crosswise grooves of different depth

Four slits with crosswise grooves of different depth were explosion tested and compared to an undamaged slit.

- Temperature measurements showed that the combustion products that flow out of the slit with multiple crosswise grooves are lower than for undamaged slits, except the slit with the smallest depth.
- The MESG values and the depths of the crosswise grooves showed no clear correlation
- Pressure measurements showed that the pressure increased by adding crosswise grooves. This indicates that the resistance through the slit increased compared to an undamaged slit.
- The slit which had the smallest depth of 0.5 mm stood out from the other slits with crosswise grooves. The MESG value for this slit was found to be smaller than the safe gap for an undamaged slit when the ignition position was 5 mm from the gap opening. It is thought that this slit caused a mixing with the unburned gas in the secondary chamber in such a way that it resulted in a higher probability for a re-ignition.

- The MESG values for the slits with crosswise grooves were not smaller than the MESG value found at worst case scenario for an undamaged slit. The overall conclusion is that slits with crosswise grooves did not reduce the efficiency of the gap. For the slits with the deepest grooves the efficiency increased.

6 Recommendations for Further Work

Rusted flame gap surfaces

Experiments on the rusted slits were not conducted at the worst case scenario in this work. It could be interesting to do experiments under these conditions to see if there are any differences in the results.

Mechanically damaged flame gaps

Due to ethylene being highly reactive it seems from this work that a certain degree of turbulence gives favorable conditions for re-ignition in the secondary chamber. It could be interesting to investigate if there are other surface configurations that decrease the efficiency of the flame gap. Some surface configurations could be:

- Crosswise grooves of different width
- One single crosswise groove
- Lengthwise grooves in relation to the flow, both multiple and single
- Random scratches from a tool typically used for maintenance of flameproof enclosure

From this work it was also shown that adding crosswise grooves changes the optimal ignition position, and that grooves create different degrees of turbulence. It is therefore recommended to investigate the optimal ignition position for each damaged slit to ensure that the experiments are conducted at worst case scenario.

Ethylene/Air concentration and other gases

A simplified approach to find the most dangerous concentration of ethylene in air for a re-ignition in the secondary chamber was conducted in this work. A more comprehensive research by finding the safe gap for different concentration, and also investigate a wider range of concentrations would give a more reliable indication of the most dangerous concentration. It would also give more information about the pressure development.

Other gas mixtures which are more representative of what is found in the industry were flameproof enclosures are used could be the next step in testing other gases.

Experiments

A Schlieren system could be used to investigate how the turbulence develops in the secondary chamber when roughness is added to the flame gap surface. It could also be interesting to compare Schlieren photographs of the primary chamber and the secondary chamber when different gases are used.

Improvements of the PRSA

Even though the Plane Rectangular Slit is a reliable apparatus it could use some improvements:

- Pressure transducers at several points in the primary chamber
- Pressure transducers in the secondary chamber

- Thermocouples better suited to measure the temperature in the hot jet
- Create a less time consuming way to change the gap width

Simulations

Simulations of the surface roughness effect on the maximum experimental safe gap have been performed for propane/air gas explosions. It could be interesting to do simulations with a more reactive gas like ethylene.

References

- AS, Y. P. (2007). "Gassfarer og gassikkerhet."
- Bardal, E. (2004). Corrosion and protection. London, Springer.
- Beyer, M. (1996). Über den Zünddurchschlag explodierender Gasgemische an Gehäusen der Zündschutzart 'Druckfeste Kapselung'. VDI Reiche.
- Bjerketvedt, D., J. R. Bakke, et al. (1997). "Gas explosion handbook." Journal of Hazardous Materials **52**(1): 1-150.
- Ceylan, K. and G. Kelbaliyev (2003). "The roughness effects on friction and heat transfer in the fully developed turbulent flow in pipes." Applied Thermal Engineering **23**(5): 557-570.
- Eckhoff, R. K. (2005). Explosion hazards in the process industries. Houston, TX, Gulf Pub.
- Einarsen, R. I. (2001). Experimental determination of holes and slits in flameproof enclosures, for preventing transmission to external explosive gas clouds. Cand.Scient, University of Bergen.
- Elsebutangen, O., Ed. (1997). Electrical Installations in Hazardous Areas. Skien.
- Frank-Kamenetskii, D. A. (1955). "Diffusion and heat exchange in chemical kinetics. ." Princeton university Press.
- Grov, A. (2010). An experimental study of the influence of major damage of flame gap surface in flameproof apparatus on the ability of the gaps to prevent gas explosion transmission. Master in science University of Bergen.
- Henden, M. J. H. (2011). Minimum ignition energy of propane and ethylene in atmospheres of various O₂/N₂ ratios. Master of Science, University of Bergen.
- IEC (2010). IEC 60079-20-1: Explosive atmospheres - Part 20-1: Material characteristics for gas and vapour classification - Test methods and data.
- IEC (2011). IEC 60079-1 Ed. 7.0: Explosive atmospheres - Part 1: Equipment protection by flameproof enclosures "d".
- Kalvatn, I. (2009). Experimental investigation of the optical measurement method for detecting dust and gas flames in a flame acceleration tube. Master Sc. Master, University of Bergen.
- Kanury, A. M. (1975). Introduction to combustion phenomena : (for fire, incineration, pollution and energy applications). New York ; London, Gordon and Breach.
- Larsen, Ø. (1998). A Study of Critical Dimensions of Holes for Transmission of Gas Explosions and development & Testing of a Schlieren System for Studying Jets of Hot Combustion Products. Cand.Scient., University of Bergen.
- Larsen, Ø. and R. K. Eckhoff (2000). "Critical dimensions of holes and slots for transmission of gas explosions: Some preliminary results for propane/air and cylindrical holes." Journal of Loss Prevention in the Process Industries **13**(3-5): 341-347.
- Lee, J. H. S. (2009). Fundamentals of Explosion.

- McCabe, W. L., P. Harriott, et al. (2005). Unit operations of chemical engineering. Boston, McGraw-Hill.
- McCabe, W. L., J. C. Smith, et al. (2005). Unit operations of chemical engineering. Boston, McGraw-Hill.
- Opsvik, H. E. Z. (2010). Experimental investigation of the influence of mechanical and corrosion damage of gap surfaces on the efficiency of flame gaps in flameproof apparatus. Master Sc. Master, University of Bergen.
- Petroleum Safety Authority Norway, P. (2009). Trends in Risk Level in the Petroleum Activity on the Norwegian Continental Shelf. Ø. Tuntland: 36.
- Phillips, H. (1972). "Ignition in a transient turbulent jet of hot inert gas." Combustion and Flame **19**(2): 187-195.
- Phillips, H. (1988). The Safe Gap: Effect of explosion pressure. IEE Conference Publication London: 5.
- Redeker, T. (1981). Classification of flammable gases and vapours by the flameproof safe gap and the incendivity of electrical sparks, Physikalische Technische Bundesanstalt, Heat Division, Braunschweig.
- Solheim, F. (2010). An Experimental Investigation of the Influence of Mechanical Damage, Rust and Dust on the Ability of Flame Gaps to Prevent Gas Explosion Transmission. Master of Science, University of Bergen.
- Tennekes, H. and J. L. Lumley (1972). A first course in turbulence. Cambridge, Mass., MIT Press.
- Turns, S. R. (2012). An introduction to combustion : concepts and applications. New York, McGraw-Hill Higher Education.
- Warnatz, J., U. Maas, et al. (2006). Combustion : physical and chemical fundamentals, modeling and simulation, experiments, pollutant formation. Berlin ; London, Springer.
- Williams, F. A. (1985). Combustion theory : the fundamental theory of chemically reacting flow systems. Menlo Park, Calif., Benjamin/Cummings Pub. Co.
- Zabetakis, M. G. (1965). Flammability characteristics of combustible gases and vapors, U.S. Dept. of the Interior, Bureau of Mines; [for sale by the Superintendent of Documents, U.S. Govt. Print. Off.

Appendix A Experimental apparatus and procedures

A-1 Equipment data

Equipment	Type
Gas Analyzer	Servomex 4200
Computer	Dell Latitude D630
DAQ	NI USB 6009
Pressure transducer	Kistler 701A
Charge Amplifier	5015A0000
Spark generator	Tailor made
Thermocouples	Tailor made (Appendix C-2)
Test gas	Ethylene
Experimental Apparatus	Plane Rectangular Slit Apparatus
Camera	Casio Exilim EX-F1

A-2 Experimental procedure - The Plane Rectangular Slit Apparatus

A-2.1 Adjusting Procedure-gap opening in the PRSA

From (Grover 2010)

1. Remove the external chamber, by turning the whole chamber counter clockwise.
2. Remove the top of the primary chamber where the flame gap is located.
3. Locate the distance "shims" in both sides through the gap (shown Figure A-1) make sure that the distance "shims" are through the whole gap width, to ensure uniform gap opening.
4. Fasten the two screws in the top of the gap (shown in Figure A-1 and Figure A-2), with a torque of 20 cNm.
5. Fasten the four screws at the start of the gap with a torque of 20 cNm (shown in Figure A-3 Figure A-4).
6. Fasten the six screws on the bottom of the gap with a torque of 1 Nm.

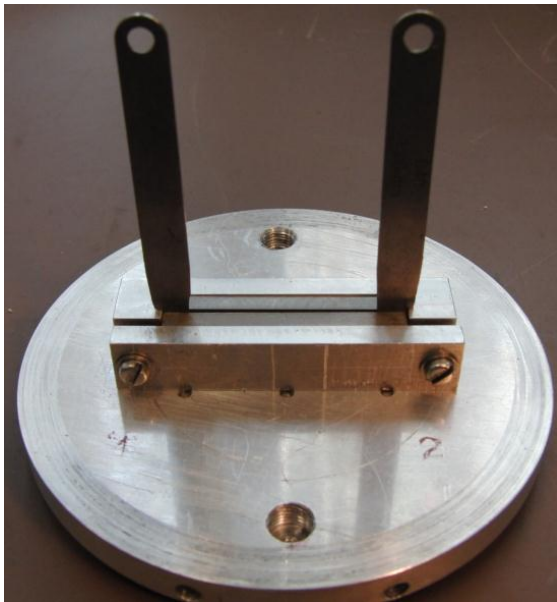


Figure A-1 Photograph of the upper part of the flame gap in the PRSA, with distance "shims" placed, the gap is fastened with a small torque applied on the screws seen in the photograph

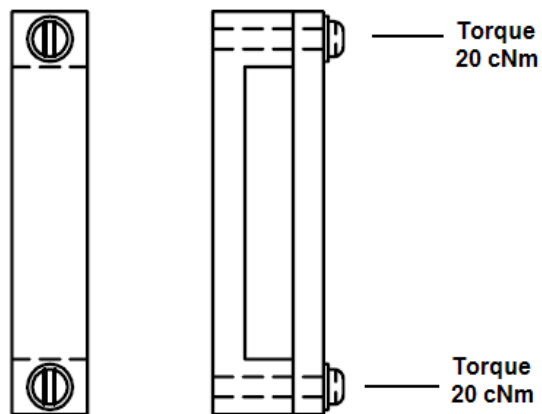


Figure A-2 Drawing of the clamp in the upper part of the flame gap, with the two screws that must be fastened with a torque of 20 cNm

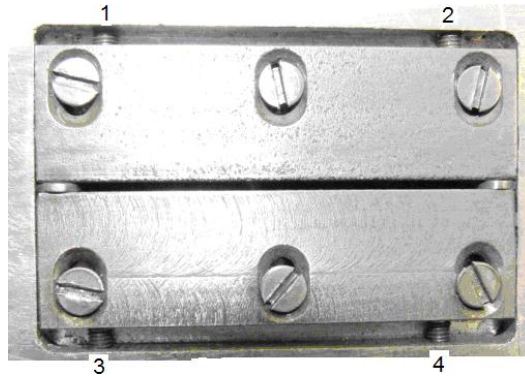


Figure A-3 Photograph of the lower part of the flame gap in the PRSA, this is the part which is inside the primary chamber. The numbers 1-4 on the photograph is the screws which are tightened with the same torque as the screws in the upper part of the flame gap, ensuring a uniform gap opening over the whole width of the gap. On the sides of the flame gap the distance "shims" can be seen on the side of the slit. From (Grovs 2010)

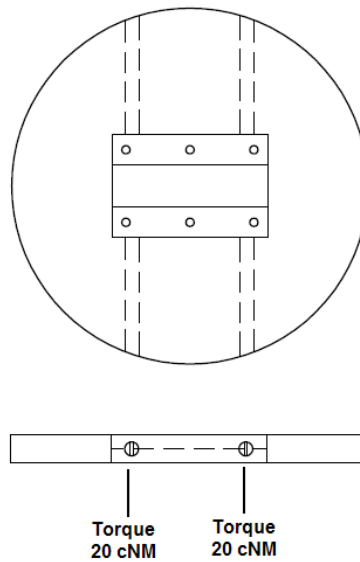


Figure A-4 Drawing of the lower part of the flame gap inside the primary chamber of the PRSA. The drawing shows where the screws clamp the gap together on the position where the distance "shims" are located. From (Solheim 2010)

A-2.2 Experimental procedure



Figure A-5 Closing valves Plane Rectangular Slit Apparatus (PRSA)

The reference values in the procedure with respect to flow are based on calculations given in Appendix B-2 and the most incentive concentration.

1. Install the plastic membrane on the top of the apparatus.
2. Open valves 1, 2, 4 and 5, see Figure A-5.
3. Set the air pressure to 1 bar
4. Start the pump on the Servomex Gas Analyser
5. Open the valve for the gas supply.
6. Adjust the air flow to 2.5 l/min and the extra flow meter (shown in Figure A-7) to approximately 45.
7. The maximum flow of the gas to be analyzed is 100 ml/min
8. Monitor the oxygen level and adjust the extra flow meter for HC up/down carefully to achieve 19.55 vol. %. Allow the analyzer to stabilize.
9. Close the valves (1, 2, 4 and 5), see Figure A-5
10. Stop the pump
11. Turn Arrow 1 on the gas analyzer to “Exhaust fan”, see Figure A-6
12. Close the extra flow meter.
13. Activate the spark generator
14. Activate the Labview program to measure the pressure and temperature
15. Wear ear protection
16. Secure the area
17. Trigger the spark by using the “remote”
18. Flush with air prior to new experiments, valve 3 Figure A-5
19. When the experiments are completed, close the gas supply and air supply

A-2.3 Calibration procedure

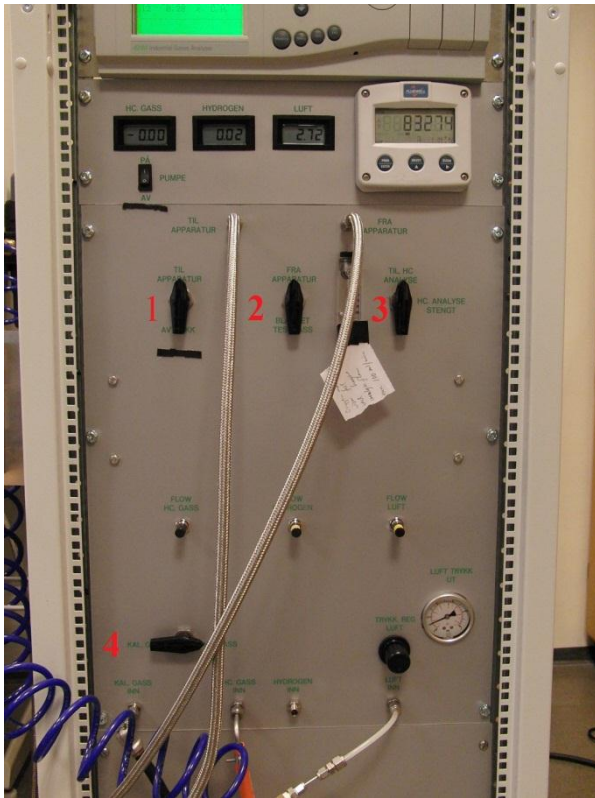


Figure A-6 Servomex Gas Analyser.

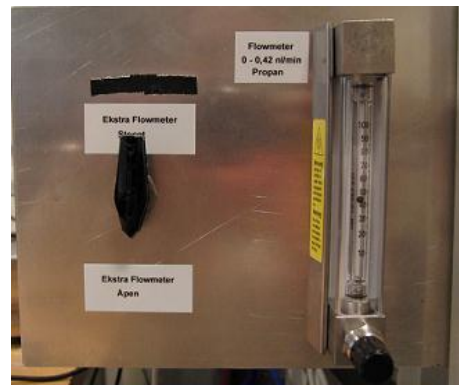


Figure A-7 Extra flow meter, placed to the left on the Servomex Gas Analyser

The gas analyzer has to be calibrated before use. The procedure is as follows:

1. Display mode must be “measure”
2. Set arrow 1 to “exhaust fan”, see Figure A-6.
3. Set arrow 2 to “mixed test-gas”
4. Set arrow 3 to “HC analysis”
5. Set arrow 4 to “Calibration gas”
6. Press the following buttons quickly: “Enter”- “quit”- “▶”- “measure”- “▲”- “menu”
7. Press enter when the mark is on “Calibration”
8. Password is 1812
9. Turn the pump on
10. Choose manual calibration
11. Choose for oxygen calibration or propane
12. Choose for high or low values of the gas to be calibrated
13. Write the percentage number of the gas in the field to the left
14. The number to the right is percentage the analyzer measures. Wait for it to stabilize.
15. The gas analyzer is now ready to be calibrated. Mark the letter ”Y”(yes) and press “enter”.

Calibration of 0% oxygen

Nitrogen with quality 5.0 is used as the calibration gas for 0% oxygen. The gas is sent into the inlet showing " calibration gas inlet". In step 12, chose to calibrate for low values of oxygen, and write in the calibration to be 0 %.

Calibration of high values of oxygen

According to the designer of the Servomex Gases Analyser, it is sufficient to calibrate for high values of oxygen with the air supply, assuming a level of 20.95vol.% oxygen in air. The only difference in the calibration procedure is that arrow 4 must be towards " HC-gas" when performing the calibration. In step 12, chose to calibrate for high values of oxygen, and write in the calibration to be 20.95%.

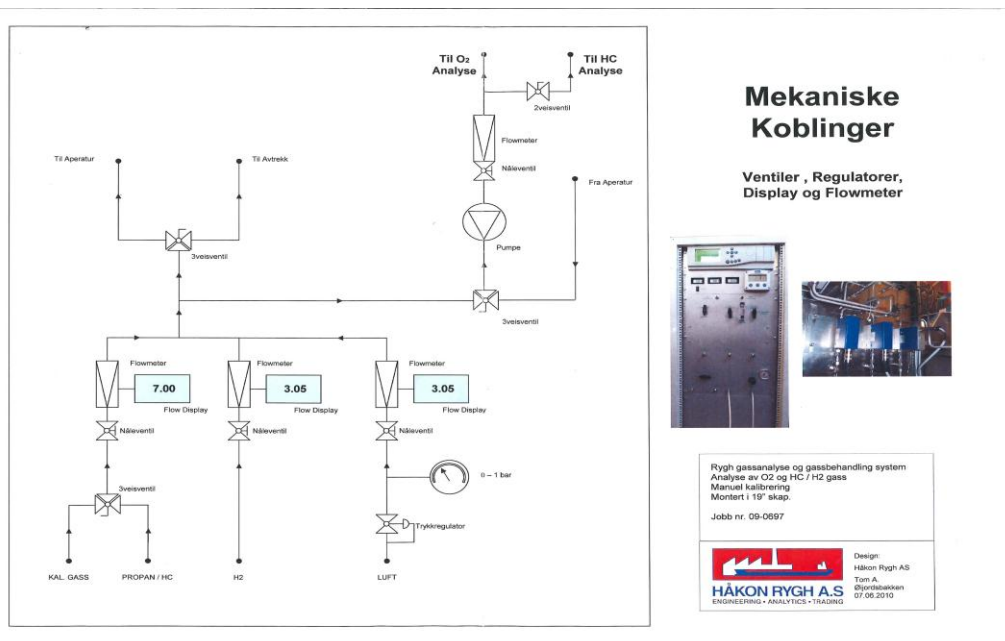


Figure A-8 Wiring diagram providing an overview of the gas analyser.

A-2.4 Data Acquisition System

Based on (Opsvik 2010)

A simplified user guide for the Labview program for running the experiment

A program is made, based on Labview, in order to measure the temperature and the pressure. Figure A-10 and Figure A-11 show the main dialog boxes. Press the buttons marked with a red circle to measure the pressure and temperature, see. After every experiment it is important that the file name for the logging file is saved. This is done via the file path dialog box.

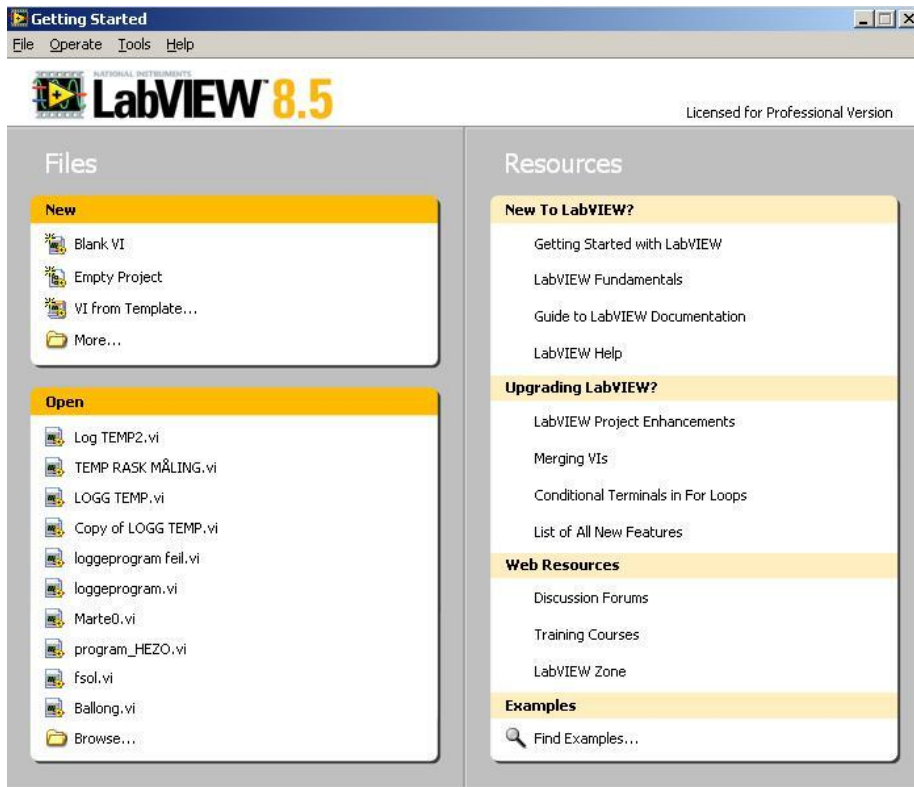


Figure A-9 Initial Labview dialog box

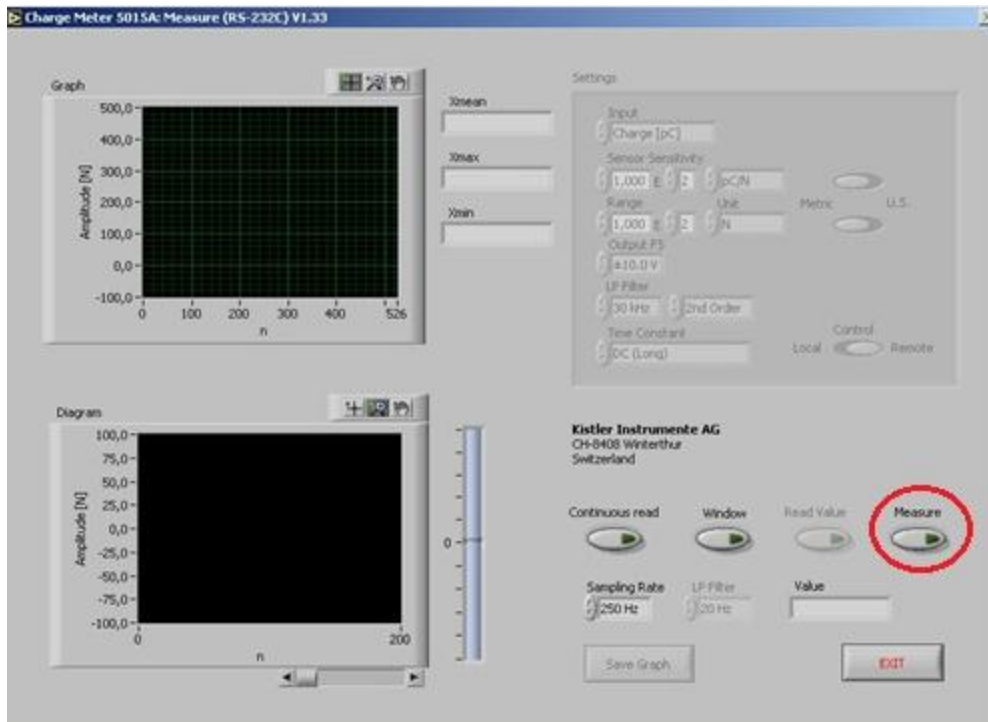


Figure A-10 Main Labview dialog box for pressure measurements.

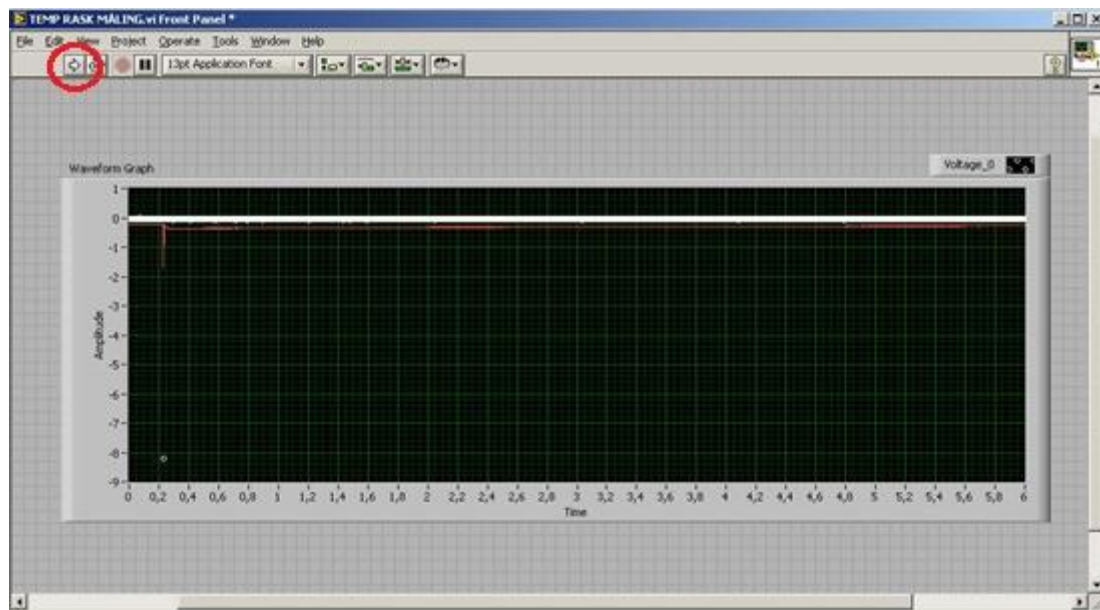


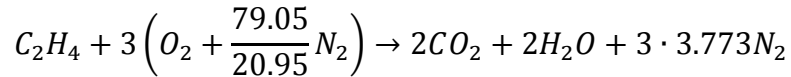
Figure A-11 Main Labview dialog box for temperature measurements.

Appendix B Calculations

B-1 Calculation of vol. % O₂ in a mixture of ethylene and air

Vol. % oxygen had to be calculated for the different ethylene/air mixtures that were investigated due to the gas analyzer only measure the propane and the oxygen concentration in a mixture. It is assumed that air contains 20.95 vol. % O₂ and 79.05 vol. % N₂ in the following calculations.

Stoichiometric



$$x = nC_2H_4$$

$$y = nO_2$$

$$z = nN_2$$

$$\frac{x}{y} = \frac{1}{3} \rightarrow x = 0.333y$$

$$z = 3.762y$$

$$0.333y + y + 3.773y = 100$$

$$y = 19.58$$

$$x = 6.52$$

Stoichiometric concentrations: 6.52 vol. % C₂H₄ and 19.58 vol. % O₂

6.0 vol. % C₂H₄

$$\frac{94.00 \text{ vol. \% air}}{100 \text{ vol \% air}} \cdot 20.95 \text{ vol. \% O}_2 = 19.69 \text{ vol. \% O}_2$$

6.2 vol. % C₂H₄

$$\frac{93.80 \text{ vol. \% air}}{100 \text{ vol \% air}} \cdot 20.95 \text{ vol. \% O}_2 = 19.65 \text{ vol. \% O}_2$$

6.5 vol. % C₂H₄

$$\frac{93.50 \text{ vol. \% air}}{100 \text{ vol. \% air}} \cdot 20.95 \text{ vol. \% O}_2 = 19.58 \text{ vol. \% O}_2$$

6.6 vol. % C₂H₄

$$\frac{93.40 \text{ vol. \%air}}{100 \text{ vol. \%air}} \cdot 20.95 \text{ vol. \%O}_2 = 19.57 \text{ vol. \%O}_2$$

6.7 vol. % C₂H₄

$$\frac{93.30 \text{ vol. \%air}}{100 \text{ vol. \%air}} \cdot 20.95 \text{ vol. \%O}_2 = 19.55 \text{ vol. \%O}_2$$

6.8 vol. % C₂H₄

$$\frac{93.20 \text{ vol. \%air}}{100 \text{ vol. \%air}} \cdot 20.95 \text{ vol. \%O}_2 = 19.53 \text{ vol. \%O}_2$$

7.0 vol. % C₂H₄

$$\frac{93.00 \text{ vol. \%air}}{100 \text{ vol. \%air}} \cdot 20.95 \text{ vol. \%O}_2 = 19.48 \text{ vol. \%O}_2$$

B-2 Calculation of flow ethylene into the PRSA

In the experiments the flow of air was held constant to 2.5 liter/min. The extra flow meter to the left on the gas analyzer was used to measure the flow of ethylene, see Figure A-7. The range from 0-100 on the flow meter equals 0-0.42 liter/min. The flow for achieving the desired concentration of ethylene is calculated by the following procedure. The example is calculated for 6.2 vol. % ethylene.

$$\frac{x \text{ liter/min}}{(2.5 + x) \text{ liter/min}} \cdot 100\% = 6.2 \%$$

$$100 \cdot x = 6.2 \cdot (2.5 + x)$$

$$x = 0.165 \text{ liter/min}$$

$$\frac{4.2 \text{ liter/min}}{100} = 0.0042 \text{ liter/min}$$

Extra flowmeter has to be set to:

$$\frac{0.165 \text{ liter/min}}{0.0042 \text{ liter/min}} = 39.3$$

The same method is used to calculate for other concentration.

Vol.%C ₂ H ₄	Flow [liter/min]	Extra flowmeter
6.20	0.165	39.30
6.50	0.174	41.40
6.60	0.177	42.00
6.70	0.179	42.60
6.80	0.182	43.40
7.00	0.188	44.70

Appendix C Experimental equipment

C-1 High speed camera

From (Solheim 2010)



Figure C-1 Casio Exilim EX-F1

The camera used in the present experimental work is a Casio Exilim EX-F1. It's a six-megapixel SLR-style camera with a 12x optical zoom lens. It has an ultra-high-speed CMOS sensor and LSI image processor and other speed enhancements giving it the ability to shoot full-resolution 2816 x 2112 pixel stills at 60 frames a second with a maximum shutter speed of 1/40,000th of a second, or to shoot video at 1,200 frames per second, allowing slow-motion shooting at up to 40x reduced speed.

C-2 Thermocouples

From (Solheim 2010)

A thermocouple consists of a junction of two different metals. The junction creates a small voltage that increases with temperature. There is a variety of different thermocouples and they are classified by which materials the junction is made of. The most common type of thermocouples is type k, which is used in this project, where the two materials in use are Nickel-Chromium and Nickel-Aluminum. Its temperature range is from -200 °C to 1100 °C, its sensitivity is approximately 41 $\mu\text{V}/^\circ\text{C}$ and they got an accuracy of about ± 2.5 °C. The thickness of the metal wires is 0.3 mm.

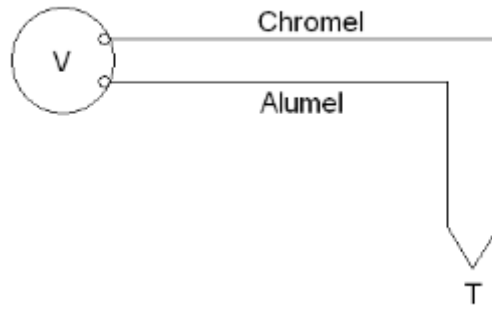


Figure C-2 Schematic of temperature measurement using a voltmeter and a thermocouple.
From(Kalvatn 2009)

Appendix D Different measurement data from experiments performed in the present work

An excerpt of the experimental data is presented in this appendix.

Experimental data from experiments prior and after rust

Preliminary experiments		
Date	14.02.2012	
Surface configuration	Undamaged	
Ignition position, Yi [mm]	14	
Vol. % ethylene	6,52	
Gap opening, Xi [mm]	Pmax [barg]	Re-ignition
0,66	1,50	No
0,66	1,50	No
0,66	1,50	No
0,67	1,48	No
0,67	1,48	No
0,67	1,48	No
0,68	1,52	No
0,69	1,49	No
0,69	1,50	No
0,69	1,48	No
0,69	1,47	No
0,70	1,60	No
0,70	1,61	No
0,70	1,59	No
0,70	1,61	No
0,71	1,48	No
0,71	1,49	Yes

		Undamaged, date 15.02.2012- 16.02.2012		Rusted slits, Date 29.04.2012- 30.04.2012	
Gap opening, Xi [mm]	Ignition position, Yi [mm]	Pmax [barg]	Re-ignition	Pmax [barg]	Re-ignition
0,68	14	1,63	No	3,77	No
0,68	14	1,63	No	3,48	No
0,68	14	1,62	No	3,39	No
0,68	14	1,64	No	3,32	No
0,68	14	1,65	No	3,33	No
0,68	14	1,62	No	3,52	No
0,68	14	1,63	No	3,51	No
0,68	14	1,62	No	3,51	No
0,68	14	1,63	No	3,49	No
0,68	14	1,64	No	3,49	No
Mean		1,63		3,48	
0,69	14	1,58	No	3,82	No
0,69	14	1,60	No	3,57	No
0,69	14	1,60	No	3,51	No
0,69	14	1,60	No	3,49	No
0,69	14	1,61	No	3,46	No
0,69	14	1,58	No	3,46	No
0,69	14	1,59	No	3,43	No
0,69	14	1,6	No	3,38	No
0,69	14	1,6	No	3,4	No
0,69	14	1,61	No	3,39	No
Mean		1,60		3,49	
0,7	14	1,53	Yes	3,77	No
0,7	14	1,54	Yes	3,52	No
0,7	14	1,52	No	3,46	No
0,7	14	1,54	No	3,41	No
0,7	14	1,54	No	3,37	No
0,7	14	1,53	No	3,39	No
0,7	14	1,54	No	3,4	No
0,7	14	1,54	No	3,38	No
0,7	14	1,53	No	3,34	No
0,7	14	1,54	No	3,38	No
Mean		1,54		3,44	

		Undamaged, date 15.02.2012- 16.02.2012		Rusted slits, Date 29.04.2012- 30.04.2012	
Gap opening, Xi [mm]	Ignition position, Yi [mm]	Pmax [barg]	Re-ignition	Pmax [barg]	Re-ignition
0,71	14	1,48	No	3,83	No
0,71	14	1,49	Yes	3,54	No
0,71	14	1,49	No	3,41	No
0,71	14	1,49	Yes	3,39	No
0,71	14	1,46	No	3,36	Yes
0,71	14	1,49	Yes	3,35	Yes
0,71	14	1,48	Yes	3,34	No
0,71	14	1,49	No	3,33	No
0,71	14	1,48	Yes	3,32	No
0,71	14	1,49	Yes	3,34	Yes
Mean		1,48		3,42	
0,72	14	1,60	Yes	4,07	No
0,72	14	1,57	No	3,82	No
0,72	14	1,58	No	3,62	No
0,72	14	1,58	Yes	3,56	No
0,72	14	1,56	Yes	3,54	No
0,72	14	1,54	Yes	3,5	No
0,72	14	1,57	Yes	3,49	No
0,72	14	1,57	Yes	3,49	No
0,72	14	1,54	Yes	3,48	No
0,72	14	1,54	Yes	3,48	No
Mean		1,57		3,61	
0,75	14	1,56	Yes	3,93	No
0,75	14	1,37	Yes	3,25	No
0,75	14	1,37	Yes	3,17	No
0,75	14	1,56	Yes	3,16	Yes
0,75	14	1,56	Yes	3,11	No
0,75	14	1,50	Yes	3,11	Yes
0,75	14	1,56	Yes	3,09	Yes
0,75	14	1,40	Yes	3,10	Yes
0,75	14	1,40	Yes	3,10	Yes
0,75	14	1,49	Yes	3,07	Yes
Mean		1,48		3,21	

Pressure measurements at different ignition position for an undamaged slit with constant gap opening

Date	26.03.2012				
Surface configuration	Undamaged				
Gap width Xi [mm]	0,69				
Vol. % ethylene	6,7				
Ignition position [mm], Yi	Pmax [barg]	Re-ignition	Ignition position [mm], Yi	Pmax [barg]	Re-ignition
5	3,29	No	10	3,29	No
5	3,31	No	10	3,31	No
5	3,32	No	10	3,32	No
5	3,28	No	10	3,30	No
5	3,31	No	10	3,30	No
5	3,32	No	10	3,32	No
5	3,32	No	10	3,29	No
5	3,29	No	10	3,33	No
5	3,31	No	10	3,32	No
5	3,30	No	10	3,31	No
Mean	3,31		Mean	3,31	

Date	26.03.2012				
Surface configuration	Undamaged				
Gap width Xi [mm]	0,69				
Vol.% ethylene	6,7				
Ignition position [mm], Yi	Pmax [barg]	Re-ignition	Ignition position [mm], Yi	Pmax [barg]	Re-ignition
14	3,53	No	20	3,51	No
14	3,58	No	20	3,51	No
14	3,32	No	20	3,52	Yes
14	3,35	No	20	3,50	No
14	3,28	No	20	3,52	Yes
14	3,34	No	20	3,51	Yes
14	3,33	No	20	3,54	No
14	3,33	No	20	3,56	No
14	3,31	No	20	3,55	Yes
14	3,33	No	20	3,57	No
Mean	3,37		Mean	3,53	

Date	22.03.2012				
Surface configuration	Undamaged				
Gap width Xi [mm]	0,69				
Vol.% ethylene	6,7		Date 02.04.2012		
Ignition position [mm], Yi	Pmax [barg]	Re-ignition	Ignition position [mm], Yi	Pmax [barg]	Re-ignition
25	3,60	No	30	3,34	No
25	3,63	Yes	30	3,36	Yes
25	3,64	Yes	30	3,33	No
25	3,65	No	30	3,35	Yes
25	3,64	Yes	30	3,34	Yes
25	3,61	No	30	3,35	No
25	3,65	No	30	3,35	No
25	3,62	Yes	30	3,36	Yes
25	3,62	Yes	30	3,29	No
25	3,62	Yes	30	3,36	No
Mean	3,63		Mean	3,34	

Date	02.04.2012	
Surface configuration	Undamaged	
Gap width Xi [mm]	0,69	
Vol.% O₂	6,7	
Ignition position [mm], Yi	Pmax [barg]	Re-ignition
35	3,42	No
35	3,40	No
35	3,42	No
35	3,42	No
35	3,42	No
35	3,41	No
35	3,40	No
35	3,39	No
35	3,40	No
35	3,41	No
Mean	3,41	

Pressure measurements at constant gap opening for slits with different depth on the crosswise grooves

Date	26.04.2012		Date	26.04.2012	
Surface configuration	PH-7.2.3.		Surface configuration	PH-7.2.2	
Ignition position [mm]	5		Ignition position [mm]	5	
Gap width Xi [mm]	Pmax [barg]	Re-ignition	Gap width	Pmax [barg]	Re-ignition
0,70	3,70	No	0,70	3,53	No
0,70	3,73	No	0,70	3,56	No
0,70	3,72	No	0,70	3,54	No
0,70	3,68	No	0,70	3,54	No
0,70	3,70	No	0,70	3,58	No
0,70	3,71	No	0,70	3,56	No
0,70	3,68	No	0,70	3,56	No
0,70	3,67	No	0,70	3,56	No
0,70	3,69	No	0,70	3,55	No
0,70	3,68	No	0,70	3,53	No
Mean	3,70		Mean	3,55	

Date	28.04.2012		Date	28.04.2012	
Surface configuration	PH-7.2.1		Surface configuration	PH-7.2.0,5	
Ignition position	5		Ignition position	5	
Gap width	Pmax [barg]	Re-ignition	Gap width	Pmax [barg]	Re-ignition
0,70	3,42	No	0,70	3,45	Yes
0,70	3,45	No	0,70	3,52	Yes
0,70	3,45	No	0,70	3,54	Yes
0,70	3,45	No	0,70	3,54	Yes
0,70	3,47	No	0,70	3,54	Yes
0,70	3,51	No	0,70	3,51	Yes
0,70	3,46	No	0,70	3,5	Yes
0,70	3,45	No	0,70	3,49	Yes
0,70	3,54	No	0,70	3,52	Yes
0,70	3,51	No	0,70	3,53	Yes
Mean	3,47		Mean	3,51	

Date	28.04.2012	
Surface configuration	Undamaged	
Ignition position	5	
Gap width	Pmax [barg]	Re-ignition
0,70	3,36	No
0,70	3,36	No
0,70	3,37	No
0,70	3,36	No
0,70	3,36	No
0,70	3,37	No
0,70	3,36	No
0,70	3,35	No
0,70	3,35	No
0,70	3,36	No
Mean	3,36	

Temperature measurements for slits with crosswise grooves

Surface configuration	PH-7.2.3
Gap opening, Xi [mm]	0,7
Ignition position [mm]	5
Thermocouple position [cm]	2
Temp [°C]	Re-ignition
80,6	No
84,7	No
81,2	No
82,2	No
81,7	No
82,1	Average

Surface configuration	PH-7.2.2
Gap opening, Xi [mm]	0,7
Ignition position [mm]	5
Thermocouple position [cm]	2
Temp [°C]	Re-ignition
73,5	No
81,7	No
82,2	No
81,2	No
N/A	No
79,65	Average

Surface configuration	PH-7.2.1
Gap opening, Xi [mm]	0,7
Ignition position [mm]	5
Thermocouple position [cm]	2
Temp [°C]	Re-ignition
100,5	No
100,0	No
104,6	No
95,9	No
100,0	No
100,2	Average

Surface configuration	PH-7.2.0,5
Gap opening, Xi [mm]	0,7
Ignition position [mm]	5
Thermocouple position [cm]	2
Temp [°C]	Re-ignition
282,6	Yes
300,4	Yes
283,6	Yes
302,0	Yes
299,9	Yes
293,7	Average

Surface configuration	Undamaged
Gap opening, Xi [mm]	0,7
Ignition position [mm]	5
Thermocouple position [cm]	2
Temp [°C]	Re-ignition
175,5	No
171,4	No
165,8	No
171,4	No
165,8	No
170,0	Average